STUDY ON THE BIOCHEMICAL FUNCTION OF RECOMBINANT DELTA CLASS *DROSOPHILA MELANOGASTER* GLUTATHIONE S-TRANSFERASE 3 (DMGSTD3)

KITHALAKSHMI VIGNESVARAN

FACULTY OF SCIENCE
UNIVERSITY OF MALAYA
KUALA LUMPUR

2014

STUDY ON THE BIOCHEMICAL FUNCTION OF RECOMBINANT DELTA CLASS *DROSOPHILA MELANOGASTER* GLUTATHIONE S-TRANSFERASE 3 (DMGSTD3)

KITHALAKSHMI VIGNESVARAN

THESIS SUBMITTED IN FULFILMENT OF THE REQUIREMENTS FOR THE DEGREE OF MASTER OF SCIENCE

INSTITUTE OF BIOLOGICAL SCIENCES
FACULTY OF SCIENCE
UNIVERSITY OF MALAYA
KUALA LUMPUR

2014

UNIVERSITI MALAYA

ORIGINAL LITERARY WORK DECLARATION

Name of Candidate: **KITHALAKSHMI A/P VIGNESVARAN**

Regisration/Matric No.: **SGR100094**

Name of Degree: **MASTER IN SCIENCE**

Title of Project Paper/Research Report/Dissertation/Thesis ("this Work"):

"STUDY ON THE BIOCHEMICAL FUNCTION OF RECOMBINANT DELTA CLASS DROSOPHILA MELANOGASTER GLUTATHIONE TRANSFERASE 3 (DMGSTD3)"

Field of Study: **BIOCHEMISTRY**

I do solemnly and sincerely declare that:

(1) I am the sole author/writer of this Work,
(2) This Work is original,
(3) Any use of any work in which copyright exists was done by way of fair dealing and for permitted purposes and any excerpt or extract from, or reference to or reproduction of any copyright work has been disclosed expressly and sufficiently and the title of the Work and its authorship have been acknowledged in this Work,
(4) I do not have any actual knowledge nor do I ought reasonably to know that the making of this work constitutes an infringement of any copyright work,
(5) I hereby assign all and every rights in the copyright to this Work to the University of Malaya ("UM"), who henceforth shall be owner of the copyright in this Work and that any reproduction or use in any form or by any means whatsoever is prohibited without the written consent of UM having been first had and obtained,
(6) I am fully aware that if in the course of making this Work I have infringed any copyright whether intentionally or otherwise, I may be subject to legal action or any other action as may be determined by UM.

(Candidate Signature) Date:

Subscribed and solemnly declared before,

Witness's Signature Date:

Name: **DR ZAZALI BIN ALIAS**

Designation

ABSTRACT

Insect glutathione S- transferases (GST) have been studied extensively due to their role in insecticide resistance and oxidative stress. The conjugations of the endogenous or exogenous toxins are catalysed by nucleophilic attack provided by side chains of active residues (Tyr, Ser or Cys) located at position 5 or 6 of the N-terminal of the polypeptide. Delta class *Drosophila melanogaster* glutathione S- transferases D3 (DmGSTD3) has however a truncated N-terminal sequence (15 amino acids) suggesting the absence of the previously mentioned active residue for catalysis. Our study was to characterise the recombinant GSTD3 and investigate the role of the amino acid residue associated to catalysis of GSTD3. DmGSTD3 gene was cloned into the pET-30a and expressed in an *Escherichia coli* production system. The GSTD3 protein was purified using an anion exchange chromatography. Substrate specificity test showed that the recombinant protein was only reactive towards 1, chloro-2,4-dinitrobenzene (CDNB) (7.3807 µmol/min/mg), a common substrate for GSTs, suggesting a possible involvement of other residues in the polypeptide that contribute to the catalysis. No activity was observed with 1,2-dichloro-4-nitrobenzene, *p*-nitrophenyl chloride, *trans*-2-octenal, *trans*-2-hexanal, ethacrynic acid, trans-4-phenyl-3- butene-2-one, hexa-2,4-dienal, *trans,trans*-hepta-2,4-dienal, cumene hyperoxide, and hydrogen peroxide. The enzyme activity was optimal at pH 8.2 and at 25° C. GSTD3 enzymatic activity was inhibited by the addition of triphenyltin hydroxide whereas; no difference in activity was detected in the presence of other inhibitors like quercetin, *trans*- chalcone, tetradecanedioic acid, sebacid acid and triphenyltin acetate. Homology modelling reveals that the side chains of Tyr89 and Tyr97 were facing towards the substrate cavity, proposing their possible role in catalyzing the conjugation. The

potential Tyr residues were mutated to alanine via side directed mutagenesis. Specific activity towards CDNB lowered to half when the Tyr89 (3.51 μmol/min/mg) and Tyr97 (3.01 μmol/min/mg) were mutated individually. GSTD3 with Y97A and Y89A gave large changes in *K*m, *V*max, and *K*m/*K*cat values for GSH as compared to unmutated GSTD3 suggesting the significant role of Tyr89 and Tyr97 in the catalysis of substrate conjugation to GSH in GSTD3. The study has confirmed the limited detoxification function of GSTD3 and the importance of Tyr89 and Tyr97 in GSTD3 catalysis.

ABSTRAK

Sifat rintang terhadap racun serangga dan tekanan oksidatif telah menjadikan glutathion S- transferases (GST) daripada serangga dikaji secara meluas. Serangan nukleofilik yang disebabkan oleh rantai sisi polipeptida residu aktif (Tyr, Cys dan Ser) yang berada pada N-terminus posisi 5 atau 6 adalah pemangkin kepada proses konjugasi toksin endogenus dan toksin eksogenus. Walaubagaimanapun, ketiadaan 15 susunan amino asid pada N-terminus glutathion S- transferase kelas D3 dari *Drosophila melanogaster* (DmGSTD3) menunjukkan kehilangan residu aktif yang penting untuk proses pemangkinan. Gen DmGSTD3 telah diklon dan diekspresikan di dalam sistem *Escherichia coli* bagi mengetahui sifat enzim ini dan mencari amino asid yang bertanggungjawab dalam proses katalisis. Residu Tyr yang disyaki memainkan peranan penting telah dimutasi melalui mutagenesis arah sisi. Melalui kajian ini, protein rekombinan yang dihasilkan didapati reaktif terhadap substrat 1,kloro-2,4-dinitrobenzen (CDNB), suatu substrat umum untuk GST kelas Delta (7.3807 µmol/min/mg), sekaligus membuktikan kewujudan residu lain yang memainkan peranan dalam proses katalisis. Tiada sebarang aktiviti dikesan apabila substrat lain seperti 1,2-dikloro-4-nitrobenzen, *p*-nitrofenil klorida, *trans*-2-oktenal, *trans*-2-heksanal, etakrinic asid, trans-4-fenil-3-buten-2-one, heksa-2,4-dienal, *trans,trans*-hepta-2,4-dienal, kumene hiperoksida, dan hidrogen peroksida. Aktiviti enzim GSTD3 optimum pada suhu 25 °C dan pH 8.2. Perencatan enzim GSTD3 dikesan berlaku dengan penambahan perencat trifeniltin hidoksida, manakala tiada sebarang perencatan dikesan apabila perencat lain seperti quersetin, *trans*-calkon, tetradekandioik asid, sebasid asid dan trifeniltin asetat. Pemodelan homologi memperlihatkan rantai sisi Tyr89 dan rantai sisi Tyr97yang berhadapan dengan kaviti substrat. Dua residu ini dianggap memainkan peranan dalam proses konjugasi. Residu tirosin yang disuspek

dimutasikan ke amino asid alanin melalui teknik mutagenesis arah sisi. Aktiviti spesifik didapati berkurangan sebanyak 50% dengan enzim GSTD3 yang telah dimutasikan pada posisi Tyr89 (3.51 μmol/min/mg) dan Tyr97 (3.01 μmol/min/mg). Apabila diperbandingkan dengan GSTD3 tanpa mutasi, enzim GSTD3 bermutasi Y97A dan Y89A secara individu, memberi perubahan yang besar terhadap nilai K_m, nilai V_{max} dan nilai K_m/K_{cat} kearah GSH lalu membuktikan peranan penting residu-residu ini dalam proses konjugasi GSH untuk katalisis enzim. Kajian ini membuktikan peranan dan fungsi DmGSTD3 yang terhad untuk proses detoksifikasi dan juga kepentigan residu-residu Tyr89 dan Tyr97 yang penting untuk proses katalisis GSTD3.

ACKNOWLEDGEMENT

I would like to take this opportunity to extend my heartfelt gratitude to the lovely people around me who have been a great driving force leading to the completion of my research thesis as an fulfilment for Masters in Science.

First and foremost sincere gratitude goes to my supervisor, Dr. Zazali Alias who has been a great guide throughout my research. Besides that, as a newbie in the biochemistry filed, my research journey was smooth due to the support and freedom given by him during my learning process. My parents, Mr and Mrs Vignesvaran-Nirmala Devi, and brother Mahesvaren, also played a huge role during the 2 years of my research. It was their understanding and motivation, also financial support that kept me going.

A big shout out to my fellow labmates (E 1.2) and dearest friends, mainly; Tanusya Murali, Siti Nasuha, Kelvin Swee, Jasmin Marie, Prazanna Laxmy and Reneshwary for their never ending moral support and help. Also to the whole Lab E1.1 students, internship students and Biochemistry 3rd and 2nd year lab staff, who were very kind to me whenever I needed a helping hand.

Last but not the least, to University of Malaya for the opportunity and financial assistances; 'Skim Biasiswa University Malaya' unit and The Institute of Research Management and Monitoring for the scholarship and research grantt awarded (PV091/2011A).

LIST OF CONTENTS

Pages

LIST OF FIGURES

Pages

LIST OF TABLES

Pages

LIST OF ABBREVIATIONS AND SYMBOLS

A. aegypti	*Aedes aegytii*
A. dirus	*Aedes dirus*
A. gambiae	*Aedes gambiae*
APS	Ammonium persulphate
Arg	Arginine
Asp	Aspartate
BLAST	Basic local alignment search tool
bp	Base pair
BSA	Bovine Serum Albumin
BSP	bromosulphophthalein
CD	Circular Dichroism
cDNA	Complementary Deoxyribonucleic acid
CDNB	1,chloro-2,4-dinitrobenzene
Cys	Cycteine
D.melanogaster	*Drosophilla melaogaster*
DCNB	1,2-dichloro-4-nitrobenzene
DDT	Dichlorodiphenyltrichloroethane
DNA	Deoxyribonucleic acid
E. coli	*Escherichia coli*
EA	ethacrynic acid
EtBr	ethidium bromide
FPLC	Fast protein liquid chromatography
Glu	Glutamate
GSH	Glutathione

GST	Glutathione S- Transferase
His	Histidine
HNE	4-hydroxynon-2-enal
Ile	Isoleucine
IPTG	Isopropyl β-D-1- thiogalactopyranoside
kb	kilobase
kDa	kilo Dalton
LB	Luria Bertani
Leu	Leucine
mRNA	motichondrial Ribonucleic acid
NADPH	nicotinamide adenine dinucleotide phosphate
NBC	4-nitrobenzyl chloride
ºC	Degree Celsius
PCR	Polymerase chain reaction
Phe	Phenylalanine
rpm	Revolutions per minute
RT- PCR	Reverse transcrptase Polymerase Chain Reaction
SDS-PAGE	Sodium Dodecyl Sulphate polyacrylamide gel electrophoresis
Ser	Serine
TEMED	Tetramethylethylenediamine
Tyr	Tyrosine
wt	wildtype

1.0 INTRODUCTION

There are few genes in insects that are directly linked to the role of detoxification or insecticide resistance. The genes responsible for this defense mechanism are either coding for insect P450s, glutathione S-transferases or esterases. Different genes play key roles in different circumstances as it is the matter of biochemical fact that several of the candidate enzymes are capable of detoxifying xenobiotics since it has been observed that single metabolic genes are upregulated in resistant strains isolated from the field (Yang et al., 2007). These enzymes provide animal the means to fend off xenobiotic challenges from the environment, such as toxic plant and microbial chemicals encountered in their food or drugs, pesticides and organic pollutants (Gaelle et al., 2006). This detoxification reaction is one of the most important mechanisms for cell survival (Saisawang et al., 2012).

Glutathione S-transferase (GST) is dimeric, cytosolic, microsomal or mitochondrial, enzymes that have extensive ligand binding properties in addition to their catalytic role in detoxification. GSTs catalyse the conjugation of activated xenobiotics to reduced glutathione (GSH) (Vontas et al., 2002). GST has emerged as promising therapeutic targets due to their isoenzyme-specific overexpression in different tumors and may play a role in the etiology of other diseases (Travensolo et al., 2008). GST can also bind to hydrophobic compounds, which are not substrates associated with sequestration, storage and transportation of drugs, hormones and other metabolites (Nair and Choi, 2011). Adding to that, GSTs also have peroxidase-like activity under oxidative stress and implicated in physiological roles such as signal transduction, cell proliferation, differentiation and apoptosis. Best example would be the way GST plays a role in regulation of JNK (c-Jun N-terminal kinase) signal

transduction pathway (Udomsinpraset et al., 2004). DDT resistance in mosquitoes has also been associated with upregulation of glutathione S-transferases (Yang et al., 2007).

Inset is the most abundant species on earth. It consists of 1 million species out of 1.5 million recorded species on earth, adding to atleast 4 million insect species yet to be discovered (Ketterman et al., 2011). Insects are the major vectors of transmissible disease and pests of major crop. This gives rise to vitality of an effective insect control (Yang et.al, 2007). Insect GST has been studied extensively due to the association of insecticide resistance and GST activity (Singh et al., 2000). Insecticide resistance is a genetic phenomenon where mutations are observed to be affecting the insecticide target proteins and metabolism. Preserving the efficacy of the insecticides and the integrity of the target is vital. The understanding in insecticide resistance can help in improving future pest control (Perry et al., 2011).

GSTs have been identified in *Musca domestica*, *Drosophila melanogaster*, *Anopheles gambiae, Anopheles dirus, L. cuprina* and, *Manduca sexta*. *Drosophila* is an appropriate model to study physiological functions of many enzymes or genes of interest (Sheehan et al., 2001). A total of 42 *Drosophila* sequences predicted to contain GST protein domains are present in the genome. Till to date, no mitochondrial GSTs have been found in insects, most studies focus on cytosolic GST (Ranson et al., 2001). The presence of large numbers of GST isoforms reflects only one thing, the significant and different functions in the organisms as each expressed protein has its own unique characteristics (Saisawang et al., 2012).

This study is to find out the amino acid residues responsible for the glutathione hydrophobic binding in the GSTD3 protein. To investigate this, the DmGSTD3 protein

structure was studied and the potential amino acid residues was chosen to be mutated via side directed mutagenesis. This is in order to observe the role of the amino acid residues towards the enzyme catalytic activity.

1.1 Objectives

The objectives of this study are;

1. To clone and express DmGSTD3 *in vitro*
2. To determine the substrate specificity of GSTD3 enzyme
3. To evaluate the role of Tyr89 and Tyr97 in GST catalysis

2.0 LITERATURE REVIEW

2.1 Glutathione S-transferases

It is through the insecticide resistance studies, enzymes with insecticide metabolizing capability which is a biochemical process when insecticides are broken down into a non-toxic form was reported (Perry et al., 2011). GSTs form a group of multifunctional isoenzymes that catalyses both glutathione (GSH) dependent conjugation and reducing reactions involved in the cellular detoxification of xenobiotic and endobiotic compounds such as hormones, heme, billirubin, drugs and pesticides which often impairs the catalytic activity of enzymes (Travensolo et al., 2008).

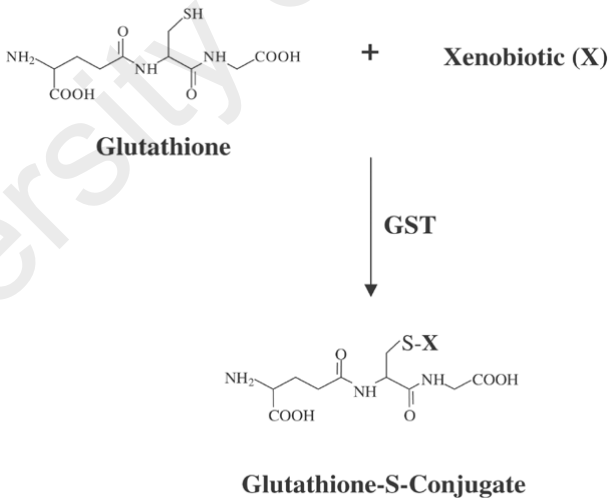

Figure 2.1 shows the glutathione conjugation to a generic xenobiotic (X) via GST results in the formation of a glutathione-S conjugate (Townsend, 2003)

In early 1965, these enzymes were named according to the substrates used in the studies by Boyland and Williams such as GSH *S*-arytransferase, GSH *S*-epoxidetransferase, GSH *S*-alkaryltransferase, GSH *S*-alkenetransferase or GSH *S*-alkyltransferase (Ketterman et al., 2011). So far, three types of GSTs have been identified; cytosolic, mitochondrial and microsomal GSTs. Microsomal GSTs comprise of integral membrane proteins which are now known as membrane-associated proteins in eicosanoid and glutathione metabolism (MAPEGs). The cytosolic and mitochondrial GST form dimers in order to become functional, but still, heterodimeric cytosolic GSTs with chains from the same classes have been indentified (Oakley, 2011).

2.2 *Drosophila melanogaster*

As for the current situation, there are 12 species of the *Drosophila* genomes have been made available along with other 7 insect species like *Aedes gambiae, Aedes aegypti, Apis mellifera, Nasonia vitripennis, Tribolium castaneum, Bombyx mori and Acyrthosipon pisum* (Ketterman et al., 2011). GST functions to confer insecticide resistance in the *Dipteran* organisms, especially delta and epsilon classes (Saisawang et al., 2012).

The work in sequencing for GST genes in fruitflies was initiated when an orthologous GST gene from the *Musca domestica* class I are found in *Drosophila melanogaster* (Ketterman et al., 2011). The GST genes are distributed on chromosome 2, 3 and X. The tandem clustering in close proximity shows that the origin of paralogous GSTs through series of tandem duplication gave rise to different isoforms with different functions (Saisawang et al., 2012). The complete *D. melanogaster* genome information gave rise to the finding of a new and most abundant insect GST

class named epsilon which plays major role in insecticide resistance (Ketterman et al., 2011).

D. melanogaster has been used as a model to study a number of the expressed products of the GST genes in relation to responses to different environmental conditions. The availability of the entire genome sequence has made it possible to study the multiple isoforms of GST in the insect using proteomics analysis (Alias and Clark, 2007). There are few key reasons and advantages in using the *D. melanogaster* as a model. This includes; ease of lab culture, complete genome sequence and short life cycle (two weeks). Besides that, the technologies available in the insect model permits systematic insecticide target and metabolism biology analysis (Perry et al., 2011).

Eventhough the *D. melanogaster* is not an insect pest, but the exposure and resistance level of insecticides has been widely observed and studied (Perry et al., 2011). The data annotations have identified 36 cytosolic DmGST genes expressing 41 types of proteins. These GSTs can be grouped into 6 classes, where at least one gene from each classs generates an alternative transcript, this is vital in more functional diversity and complexity (Saisawang et al., 2012). Delta classes GSTs are abundant in *Drosophila melanogaster* together with epsilon class (Sheehan et. el., 2001) all which have had their genome sequenced (Li et. al, 2009). Most recent studies show that the DmGST isoforms are generally expressed during the late embryonic stages (Saisawang et al., 2012). There are four DmGST genes structures that are currently available; Sigma 1, Delta1, Delta4 (Apo) and Delta4 (GTT) (Ketterman et al., 2011).

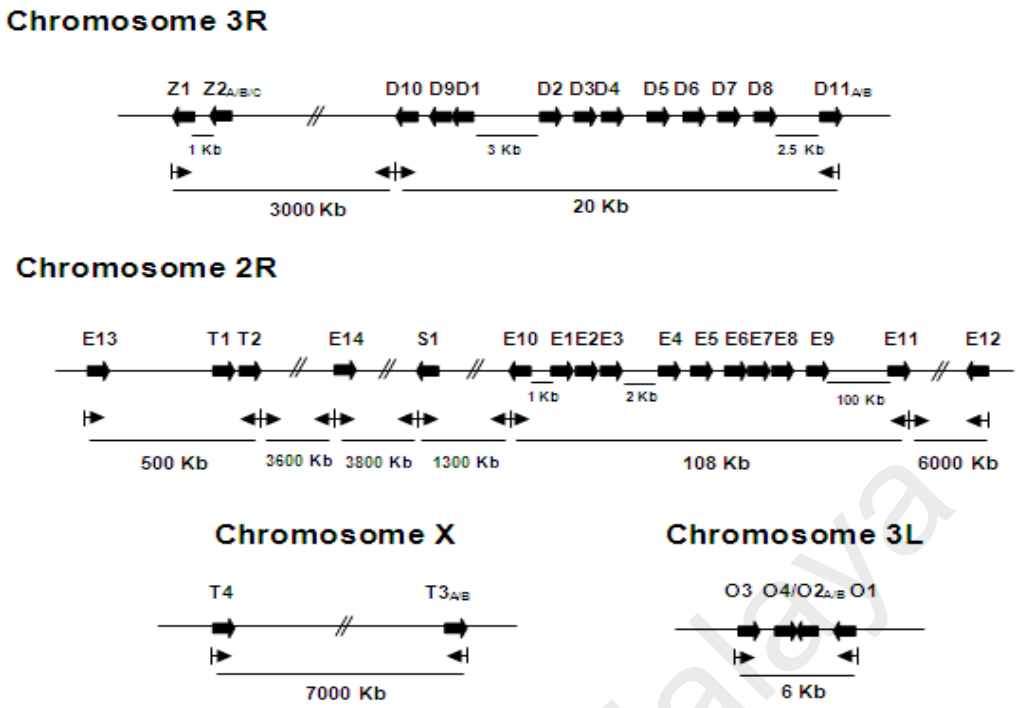

Figure 2.2 shows the genomic organization of *Drosophila* GSTs (Saisawang et al., 2012)

2.3 Classifications and nomenclature

Over 40 genes have been discovered and they can be divided into 14 distinct classes. These include the cytosolic GSTs of 7 mammalian classes; alpha, mu, pi, sigma, zeta, theta, and omega, plants classes; phi and tau; Insects classes; delta, epsilon, and bacterial class; beta (Winayanuwattikun and Kettermen, 2005; Saisawang et al., 2012) and a mitochondrial GST, known as the kappa class (Oakley, 2011). Alpha, mu, pi classes exists in vertebrates, for example, mammals and fishes (Saisawang et al., 2012). Classes like zeta, theta, sigma and omega has been said to be conserved in bilaterian animals from deuterostome and protosome lineages (Ketterman et al., 2011). Theta, omega, zeta and sigma was found to be the most ancient classes to be found in eukaryotes (Saisawang et al., 2012). The divisions are on the basis of their primary structure, immunological properties, and substrate specificities (Winayanuwattikun and

Kettermen, 2005). It is generally recognized that the protein sequence identities of GSTs from the same class should be more than 40% but less than 30% between different class GSTs (Wan et.al, 2008). In other words, the amino acids sequence appears to be relatively more conserved within the same classes (Saisawang et al., 2012).

Ketterman and group has suggested that besides the above, mentioned criteria, phylogenetic relationships, chromosome localization and structural similarities should also be exploited in classifying a GST gene (Ketterman et al., 2011). The advantage of multiple forms of GST is crucial for the evolution of the enzyme family. This GSTs superfamily evolution is strictly conserved, where alternative splicing occurs and produces broad range of mRNA diversity with vast protein product variation. The alternative splicing is the reason for the polymorphism of functionally distinct proteins. And it has to be clear to all that the enzymatic function does not correlate with any of the classification criteria (Saisawang et al., 2012).

GSTs were first grouped according to their properties like immuno-cross-reactivity or substrate specificity, but this lead to confusion when insect theta GSTs appeared to be active with CDNB contradicting to mammalian class GSTs and also only one out five omega GSTs plays a role in the pteridine eye pigments synthesis (Ketterman et al., 2011). In early studies on *Musca domestica* gave rise of two different classes of GST according to the electrophoretic group, in which a multigene family was found to be coexisting in *Drosophila* as well. It was then named the delta class in an attempt to bring the insert GSTs classification in line with the mammalian GSTs classification system (Ketterman et al., 2011).

Insect GSTs comprise of 6 classes; zeta, sigma, theta, omega, delta and epsilon. The latter two are insect specific and said to be most abundant in insects. But, the absence of a single epsilon GST in Hymenoptera, and the discovery of delta GSTs in arthropods like crustaceans doubt the previous statement (Ketterman et al., 2011). Through sequence similarities and phylogenetic analysis, it was proven that delta and epsilon class GSTs are the most closely related, whereas the sigma class is the most significantly different class with only 3-10% amino acid similarity (Saisawang et al., 2012).

Based on the phylogenetic analysis, delta and epsilon are the most closely related class with a similar structure as what shown by the structural superimposition (Ketterman et al., 2011). Saisawang et al. (2012) has also reported that omega, delta and epsilon class may have an inter-functional relationship as all three showed similar thioltransferase activity in *D. melanogaster* (Saisawang et al., 2012). The delta and epsilon GST classes have expanded independently in *D. melanogaster* and *A. gambiae*, suggesting that these enzymes play important roles in the adaptation of these species to their specific environments (Enayati et. al, 2005).

2.4 Gluthathione

Gluthathione is a tripeptide (GSH) consisting of glutamate, cycteine and glyceine (γ-glu-cys-gly). GSH serves as a cellular reductant and scavenging agent for reactive electrophilic compounds. The structural studies and activity chemistry has showed that GST bind and activates the thiol group of GSH (Dixon et al., 2010). The conjugation with the GST makes a compound more soluble as substrates for cellular export proteins. Besides this, some GSTs utilizes GSH as cofactors, not just merely as substrates alone, for example in leukotriene biosynthesis (Oakley, 2011). When GSTs are involved in conjugating acceptors with GSH, it is a compulsory requirement for the enzyme to possess the conserved serine residue at the active site; this is the region that facilitates the thiolation of the GSH anion. Besides that, GSH has also been reported to be involved in conjugating with plant metabolites without the help of GSTs (Dixon et al., 2010).

2.5 Roles of GSTs

Basically GSTs catalyze the conjugation of GSH to an array of different electrophilic compounds. It has been reported to catalyze reactions in leukotriene and in the biosynthesis of prostaglandin (Oakley, 2011). GST classes have gone through an evolutionary conservation of species diversification for millions of years which proves its involvement in fundamental roles (Ketterman et al., 2011). GST has many vital roles to play, apart from conjugation; it also functions in hormone biosynthesis, tyrosine degradation, breakdown of peroxidase, reduction of dehydroascorbate and many others (Oakley, 2011).

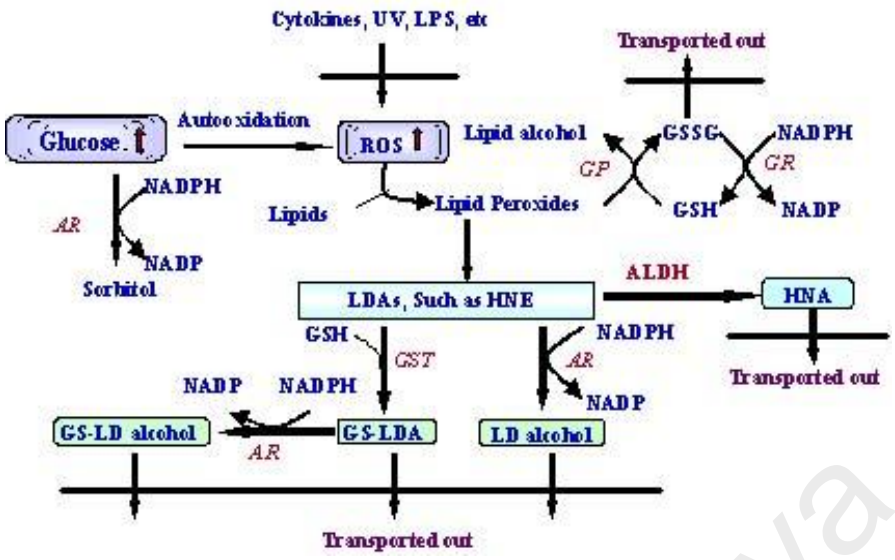

Figure 2.3 shows the role of GST in defense mechanism
Source: http://www.bmb.utmb.edu/faculty/ansari_n/

Detoxification is a very important metabolic and defense mechanism in a living organism to sustain (Oakley, 2011). The enzymatic detoxification of xenobiotics has been classified into three distinct phases which act in a tightly integrated manner. A prevalent detoxification pathway begins with phase I metabolism, the oxidation by cytochrome P450 monoxygenase (Guengerich, 1991). It is a family of microsomal proteins that are responsible for a range of reactions, of which oxidation appears to be the most important (Guengerich, 1990). The second step, phase II metabolism, involves a conjugation reaction, catalyzed by a variety of enzymes, including GSTs (Mannervik and Danielson, 1988). Phases I and II involve the conversion of a lipophilic, non-polar xenobiotic into a more water-soluble and therefore less toxic metabolite, which then can be eliminated more easily from the cell. For example, polyaromatic hydrocarbons (PAHs) which is an environment pollutant, is oxidized by CYP450s, substrates of GST.

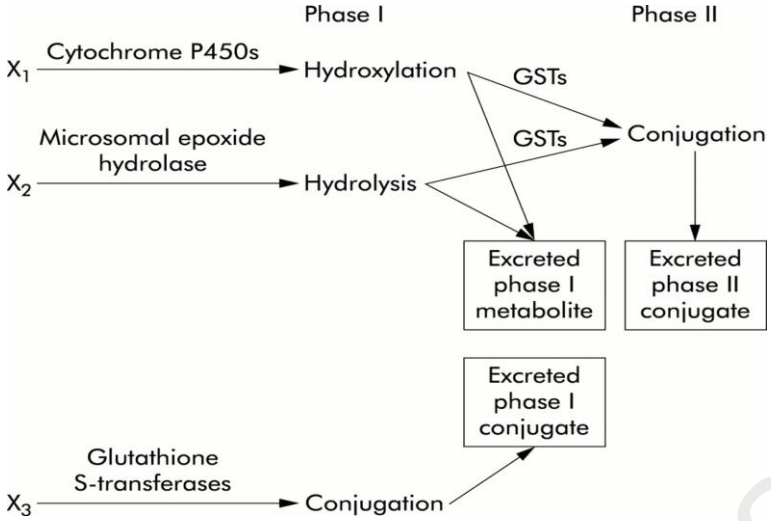

Figure 2.4 shows the overview of xenobiotic metabolism. X_1, X_2, and X_3 are different xenobiotic substrates (Sandford and Silverman, 2002)

GSTs also plays role of pharmacological interest. For example, in humans, it conjugates drugs and other xenobiotics. Not only that, the human pi-class expression is highly related with resistance towards chemotherapeutics. Clinically, GST plays an important role in chemotherapy resistance. Resistance to a range of anticancer drugs like chlorambucil can be observed through the increasing level of the pi-GST in tumor cell lines. Moreover, the GSTs dichloroacetate (DCA)-transforming activity is also an advantage in clinical treatment of the congenital lactic acidosis (Oakley, 2011).

The role of GST in lipid peroxidation is also something that needs to be highlighted. This is because the catalytic efficiency is high even when it lacks stereoselectivity. 4-hydroxynon-2-enal (HNE) is an example of a lipid peroxidation product which alpha class GST conjugates with. The GS-HNE conjugate undergoes reversible cyclization (Oakley, 2011).

Alpha and zeta classes posses GSH-dependant isomerisation activities, sigma classes are hematopoietic prostaglandin D synthase and catalyzes prostaglandin D_2, theta class shows sulfatase activity, and omega class form mixed disulfides with GSH

to catalyze reductase reactions, while beta class GSTs gives protection against chemical and oxidative stress, antimicrobial drug resistance and in catabolism of xenobiotics (Oakley, 2011).

Besides that, GSTs also play role in non conjugating roles via GSH. For example, the GSH is used as a reducing agent to catalyse the conversion of dehydroascorbate to ascorbic acid by the mixed disulphide bridge formation with the cysteine. Alternatively, serine residue at the active site mediates the reduction organic hydroperoxides to alcohols by glutathione peroxidise where the GSH instead of forming a stable conjugate with the co-substrate, undergoes oxidation to form GSSG disulfide and recycled by glutathione reductase (Dixon et al., 2010).

GST does also play a significant role in the isomerisation in tyrosine catabolism and caretenoid synthesis pathway via *cis-trans* isomerisation (Dixon et al., 2010). The zeta-class of GST known as maleylacetoacerare isomerise (MAAI) catalyzes maleylacetoacetate to fumarylacetoacetate. MAAI is the key enzyme in tyrosine and phenylalanine catabolism. The tyrosine degradation pathway due to the lack of these enzymes can cause diseases like phenylketonuria, alkaptunoria and the fatal tyrosinemia type I (Oakley, 2011).

Another interesting role of the GST is in the transport of the secondary metabolite either in order to stabilize the pathway intermediates or as protein shuttles between the synthesis and usage. GST would bind with the molecule of interest once it's transported into the cytosol and deliver it to a membrane transporter like the ABC transporter. Once delivered, the conjugation is reversed and the GSH is released and recycled. Example of such mechanism is the electrophilic oxylipins group, OPDA, a

highly reactive intermediate synthesized in the jasmonate synthesis in the choloroplast and metabolized in peroxisome. The GST enzyme helps this molecule to cross over the cytosol into the peroxisome without any modification (Dixon et al., 2010).

This explains the role of the GSTs that seem to lack the GSH-activating serine or cysteines at their active site, but still being expressed which suggest the non-catalytic role. The discovery of additional non-catalytic ligand-binding sites has also been recently reported (Dixon et al., 2010). GSTs as ligandins were first identified as cytoplasmic protein which could bind to compounds like bilirubin, heme, xenobiotics, steroids and azo-dyes; contributing to intracellular sequestration and transport. Ligandin site was discovered in rat GSTA3-3 within the two subunits cleft through affinity labeling (Oakley, 2011).

Plant GSTs was originally discovered when they exhibited the ability of conjugation and detoxification of cloro-*s*-triazine photosystem II inhibitor atrazine in maize. It was also found then that the level of GST in the domestic crop is higher compared to the competing weed plant. This explains that these enzymes are responsible in determining the differential metabolism and selectivity of major herbicides. Besides herbicide detoxification, GSTs expression has also been linked with plants responses with abiotic and biotic stress, hormones and developmental change (Dixon et al., 2010).

Insects that are vectors of agricultural pets were given more attention since GSH-dependent enzymes were observed to metabolize organophosphates and chlorines of insecticides (Ketterman et al., 2011). The role of these genes in detoxification was proven by the studies of 1, 1, 1-trichloro-2, 2-bis (ρ-chlorophenyl) ethylene resistance

in *A. aegypti* and *A. gambiae* by GSTE2. The DDT is metabolized to the non toxic 1, 1-dichloro-2, 2-bis (ρ-chlorophenyl) ethylene (DDE) through dehydrochlorination (Ayres et al., 2011). The enzyme activity was detected with similar specificity in both susceptible and resistant insects, just that in larger quantity in resistant insects. Recent studies shows, that insects have also developed resistance towards the now widely used insecticides, pyrethroids. It has been found that GSTs plays a role in contributing to the resistance by firstly binding and sequestration of the pyrethoids followed by oxidative stress response (Ketterman et al., 2011).

2.6 Structure and enzyme specificity

Although the reason of presence of the large numbers of isoforms in an organism cell is not yet known, but the prolific expression elucidates that this phenomena suggests an array of functions for these proteins (Saisawang et al., 2012). Structural studies of various GSTs show that all the structures have the same basic protein fold which consists of two domains (Armstrong, 1997). Due to the relevance to toxicology, cancer and drug metabolism, the mammalian cytosolic class GST was the first to be structurally characterized, precisely, porcine pi-class (Oakley, 2011). There are two substrate-binding cavities in GSTs known as the G-site and the H-site. The first is specific towards the glutathione (GSH) and latter for the hydrophobic electrophilic second substrate (Malena and Bengt, 2011). The GST protein forms a dimeric quaternary structure as it's essential for fully functional active sites which are from both subunits. In delta class, 25% of its active sites amino acids are from the other subunit (Ketterman et al., 2011).

There are several motifs that are adapted by the GSTs quaternary structures; some conserved in GSTs in general; some restricted certain species. The N-terminal domain adopts a βαβαββα motif, which is a thioredoxin like structure and contains GSH-binding sites (G-Sites), whereas, the C-terminal domain is a large α domain, containing five to six α-helices and hydrophobic substrate-binding sites (H-Sites) (Wan et al., 2008). The kappa class, mitochondrial GST has certain topological similarities and differences with the cytosolic enzyme. The conserved region in both cytosolic and mitochondrial GST is the cis-proline residue at the N-terminal end of the β3 that forms a hydrogen bond interaction with the amine group backbone of the GSH-cystenyl moiety (Oakley, 2011). Dimerization of two GST subunits is vital for the tertiary structure stabilization of the individual subunits. This tertiary structure is highly conserved where else the dimerization is highly specific and said to only occur between subunits from the subunits, but there are studies suggest that heterodimerization is also may preclude (Ketterman et al., 2011).

The fundamental aspect of the enzyme catalytic mechanism is how the binding interaction with GSH facilitates the nucleophilic attack. So far, catalytically active monomers have not been observed, or perhaps the appropriate conditions have not been found yet (Armstrong, 1997). In many GSTs, the catalytic function of the enzyme is said to be accomplished by a tyrosine at H-bonding distance from the sulphur of GSH. Then the reduced form of glutathione (GSH) and GST catalyse a nucleophilic attack on nonpolar compounds that contain an electrophillic carbon, nitrogen, or sulphur atom (Vuilleumier, 1997). However, the roles of several active-site residues and functional groups of GSH have been studied intensively and the conserved tyrosine/serine residue is responsible for the functional role of the protein located in the N terminal of the sequence (Winayanuwattikun and Kettermen, 2007). Structurally, the peptide is bound

in an extended conformation, with the glutamyl residue pointing down toward the dimer interface, the cysteinyl sulfur pointing to the subunit to which it bound, and the glycyl residue residing near the surface of the protein (Armstrong, 1997). There are several crucial charged/polar residues which directly interact with the GSH promoting ionization, and supported by interactions with neighboring residues. This network is important in base-assisted deprotonation model to promote the glutathione thiol group ionization. This network of residues although not identically conserved across the classes, but the network motifs are functionally conserved in the tertiary structures of different GSTs which proves the significance of the network (Ketterman et al., 2011).

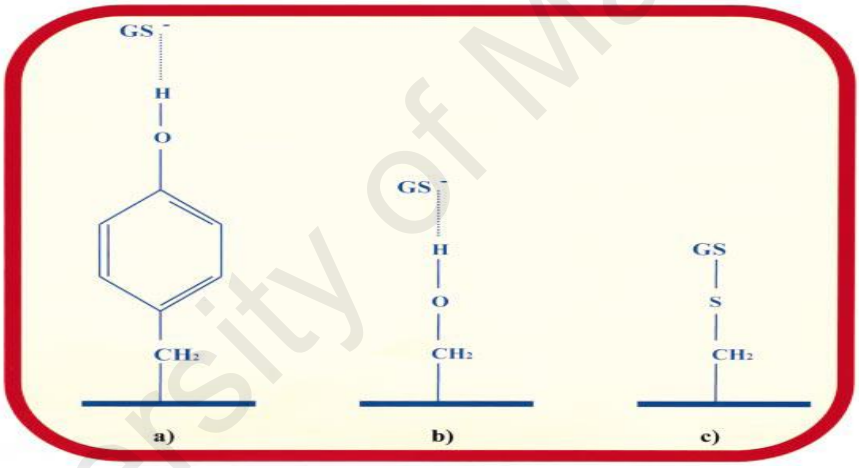

Figure 2.5 shows the active-site residues in GSTs. In most GST classes, an N-terminal tyrosine residue (*a*) interacts with GSH to stabilize the thiolate anion, with a consequent decrease in p*K*a. In the theta and possibly the zeta classes, this role is carried out by a serine residue (*b*), while in the omega and beta classes a mixed disulphide is formed with a cysteine residue (*c*) (Sheehan et al., 2001).

GST has broad and overlapping specificity. Catalytic promiscuity is displayed in the protection of cells against the challenges of a myriad of chemical electrophilic species. The residues forming the active site determine the substrate selectivity of an enzyme (Malena and Bengt, 2011). Cytosolic GSTs are active as dimers of either homogeneous or heterogeneous subunits whose molecular masses range from 23 to 28 kDa (Wan et. al, 2008). There are few GST isoforms present in each species which

carries specific physiochemical properties and substrate specificity hence suggesting the multiplicity of the enzyme (Ketterman et al., 2011). Generally, a big portion of the N-terminal domain forms the G-site which is conserved across classes, while the C-terminal forms the H-site that varies and plays a huge role in substrate selectivity hence giving the enzyme a unique physiological function (Saisawang et al., 2012). The H-site varies in the sense of structure and chemical features between different classes (Oakley, 2011). A lot of studies have been carried out at the residues forming the H-site, as it represent the first sphere of interaction with the co-substrate. This will aid in understanding the enzyme catalysis and substrate specificity (Wongsantichon et al., 2010).

Malena and Bengt (2011) carried out an investigation on point mutations in the substrate binding H-site can affect the substrate selectivity profile of the human mu class GSTs. Mutation was done to the conserved tyrosine region with a smaller amino acid residues and found that there was an enhance in activity with other epoxide substrates. Also the use of alternative substrates resulted in the identification of novel GSTs from the same parental GST but with different catalytic ability. This demonstrates the effect of evolution that gives rise to specialized functions due to the multivariate selection pressure in nature. One of the example given were like GST A4-4, which is specialized for conjugation of 4-hydroxynonenal and analogous substrates, and human GST M2-2 displaying prominent activity with ortho-quinones derived from naturally occurring catecholamine. But however, it was also reported that the evolution to a higher catalytic efficiency decreased the range of selectivity or 'promiscuity'. This was explained as that strong stabilization of the transition state for the catalyzed reaction and a given enzyme structure limited the number of alternative transition states where the active site can take in for catalysis (Malena and Bengt, 2011).

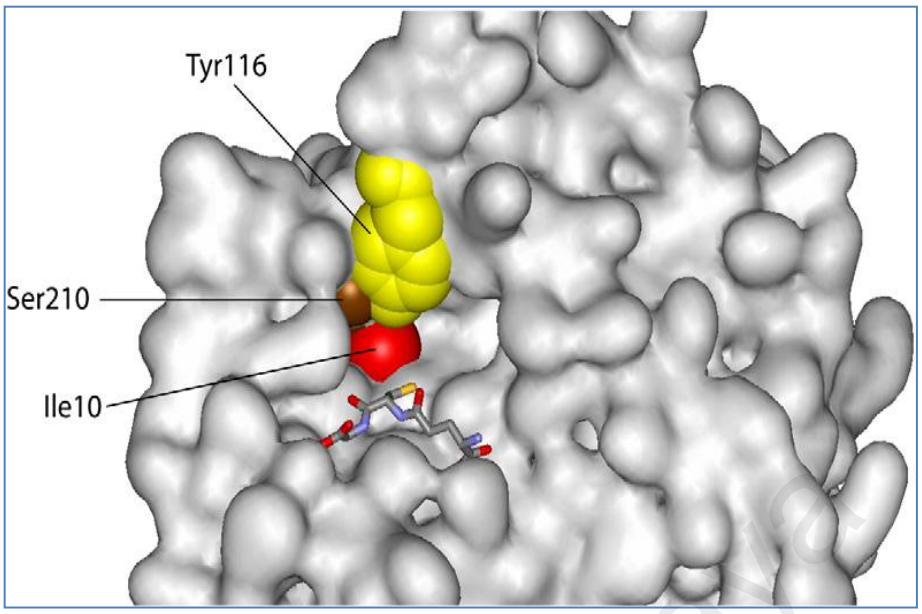

Figure 2.6 shows the active-site structure of human GST M2-2. Close-up of the monomeric GST M2 subunit (Protein Data Bank code: 2C4J) where the catalytic Tyr116 is in yellow, the hypervariable Ser210 is in brown (Thr in wild-type enzyme), and the highly conserved Ile10 is in red. Glutathione (stick) contains sulfur (yellow) to which the electrophilic group of the second substrate will bind (Malena and Bengt, 2011).

But, Oakley stated that the crystal structure of GSTA4-4 has shown that the active site residue, R15, interacts with the 4'-OH of HNE enantiomer and assist in catalysis by polarizing the group through an H-bond donation. A tyrosine, Y212, contributes a hydrogen bond to the aldehyde oxygen atom and stabilizes the enolate reaction intermediate. Besides that the Y9 residue as usual activated the GSH for the reaction with α,β-unsaturated moiety (Oakley, 2011).

As for so far, only 16 structures of insect GST is available in the RCSB Protein Data Bank out of 300 hits of GST structures, these includes 4 *Drosophila melanogaster* GST genes. Through structural superimposition it was found that delta classes GSTs are structurally similar even with 40% - 80% amino acid sequence identity (Ketterman et al., 2011).

In delta class GSTs, the first structurally concerned residue studied was Leu-103. Besides that, there are 13 residues forming a sphere, in which 6 are in the active site interacting with another 5 residues. Arg-67 particularly interacts with the γ-glutamyl of GSH and is conserved within the delta class, where as in human class, Arg-69 takes over the role of GSH binding and enzyme stabilization. A change in the Leu-103 residue has been reported to affect residues at the active sites and at the subunit-subunit interface which forms the 'clasp' motif. This 'clasp' motif also known as the 'lock-and-key' motif is strictly conserved across the insect GSTs classes. It connects the G-site of one subunit to the other, where the Phe-104 modulates the GSH binding for both subunits (Ketterman et al., 2011).

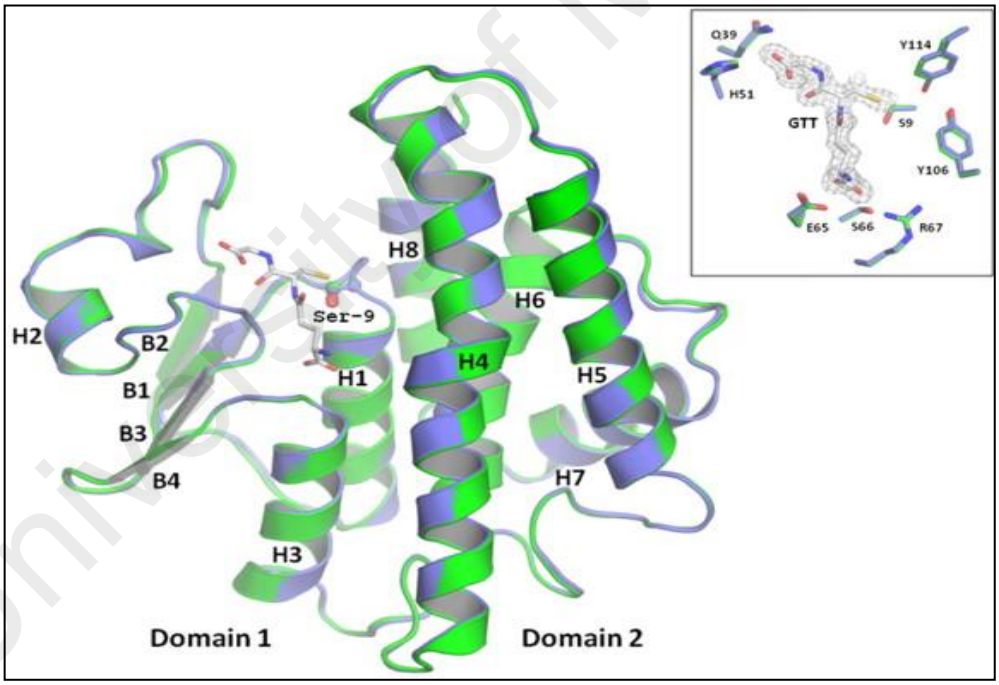

Figure 2.7 shows the dimensional structure of D10 and D10GS. Ribbon representation of D10 and D10GS are shown in blue and green color, respectively. Glutathione substrate is in stick and Serine-9 in ball-and-stick. An inset shows GSH interacting residues (Wongsantichon et al., 2012).

The aromatic motif modulates the protein structure and affects the stability as well as the active-site topology. Wongsanthichon et al. has studied on the aromatic 'zipper' in the H-site that contributes as a network of π-π aromatic interactions, where some residues directly interact with the hydrophobic substrate while others indirectly maintain the dimeric conformational structure (Wongsanthichon et al., 2010). Besides that, there are several other residues important in the structural maintenance and initial folding, like N-capping box and hydrophobic staple motifs. The N-capping box is located at the N-terminal region of α-6 helix and plays an important function in the stability of the protein. Glu-64 is a residue functionally conserved in GST delta class which directly interacts with the γ-glutamate moiety of GSH in order for the catalysis to occur and also for initial folding. Other than that, His-50 interacts with the glyceine moiety of GSH for ionization and very important in charge-sharing networks in the G-site (Ketterman et al., 2011).

For kinetic characterization of DmGSTs, CDNB conjugation has been always used as a standard assay thanks to its high GST specificity towards the substrate in general, except for zeta class, where dichloroacetic acid (DCA) assay is employed as replacement. The zeta class catalyzes the oxygenation of DCA to glyoxylic acid just like zeta classes of plants, rats and humans. Generally delta and epsilon GSTs shows greatest activity towards xenobiotics when compared to enzymes from other classes. In epsilon class, even with conserved G-site, the K_m for GSH was from 0.46 to 40.6 mM, for example DmGSTE11-11 has the highest catalytic activity towards CDNB, 1870 fold greater than the least efficient epsilon class. In delta class, DmGSTD11a-11a was reported to be the most reactive enzyme as the V_{max} is the greatest among all other GSTs. DmGSTD1-1 is the most versatile enzyme in the delta class as it can conjugate with most endogenous toxic compounds like 4-hyrdroxynoenal (4-HNE),

adrenochrome, phenethyl isothiocyanate (PEITC), prostaglandin A_2 (PGA_2) and others (Saisawang et al., 2012).

2.7 DmGSTD3

DmGSTD3 was first presumed to be a pseudogene by Toung et.al, (1993) on the basis of a sub-optimal Kozak context of the translation initiation codon, and a 15-amino acid N-terminal truncation (Alias and Clark, 2007). DmGSTD3 seems to be lacking the N-terminal sequence that includes the highly conserved tyrosine residue involved in the catalytic cycle of GSTs (Toung et al., 1993). But Sawicki et al., (2003) identified a DmGSTD3 transcript by RT- PCR which demonstrates that the gene is expressed, at least up to the stage of transcription and transcript processing. This has also been supported by Alias and Clark who noticed the extensive expression of the protein (Alias and Clark, 2007).

The roles of several active-site residues and functional groups of GSH have been studied intensively and the conserved tyrosine/serine residue is responsible for the functional role of the protein (Winayanuwattikun and Kettermen, 2007). Studies proved that DmGSTD3-3 is active towards 4-HNE, with kinetic parameters similar to those of other delta class GSTs (Sawicki et al., 2003). HNE is a secondary cytotoxic lipid peroxidation end product which acts as a signaling molecule that causes several degenerative diseases (Saisawang et al., 2012). Serine residue at position 9 has been always responsible for conjugation of GSH to xenobiotics. From bioinformatics and homology modeling analysis shows this residue is not present in GSTD3. In replacement of the function a serine residue from a distant domain of the sequence is

shown to be responsible for the catalysis. This is possible as a conformed protein somehow pointing the Serine residue forward, the inner cavity of the active site.

Demonstrating the involvement of the far distant residue in the catalysis may offer another possibility of catalysis in GST. Moreover, studies showed that the D3-D3 isoform from *Anopheles dirus,* in addition to the Ser9 residue generally regarded as involved in abstraction of a proton from the thiol group of bound glutathione, other residues act by assisting the glutamyl α-carboxyl of glutathione to participate in protein abstraction. For *A. dirus* GSTD3-D3, residues interacting with the glumate carboxyl include Ser65, Arg66 and Asp100. Homology modeling with the DmGSTD3 protein indicates the existence of homologous residues, Ser49, Arg50 and Asp84, which might participate in such reaction (Alias and Clark, 2007).

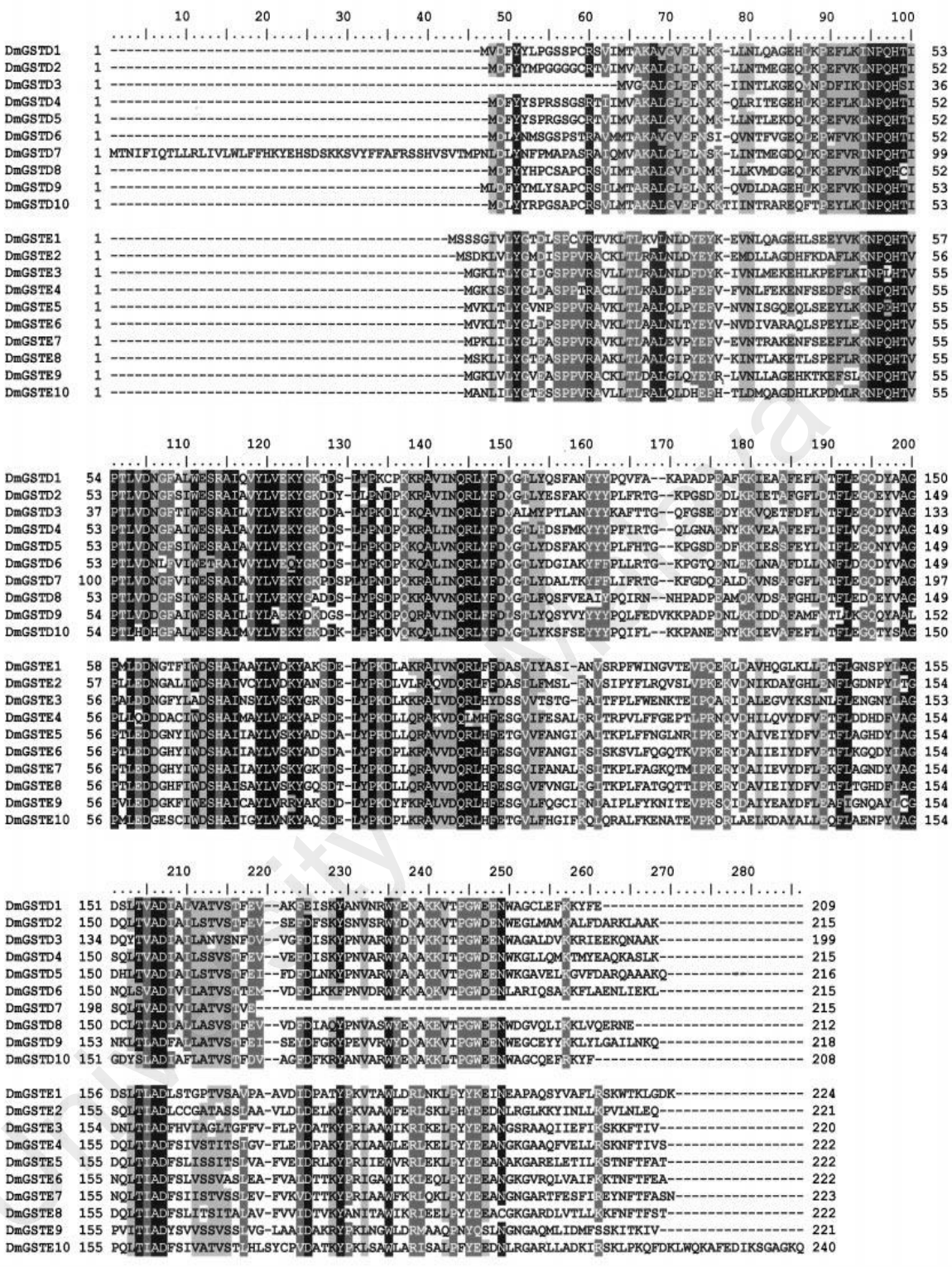

Figure 2.8 shows the alignment of the predicted protein sequences of *D. melanogaster* delta and epsilon class glutathione transferases. DmGSTD3 is found to be lacking the first 15 amino acids at the N-terminal (Sawicki et al., 2003)

2.8 Side directed mutagenesis

Side directed mutagenesis has been a valuable tool for assessing electrostatic contributions of various residues in the vicinity of the sulfur to catalysis. It often has led to the identification of residues important in the substrate specificity of GST even in the absence of three dimensional structures (Armstrong, 1997). Variations of the amino acid residues that make up the electrophilic substrate-binding site (H-site) in different isoenzymes provide the GST family with the ability to catalyze reactions toward a large number of structurally diverse substrates (Johansson and Mannervik, 2001). The importance of the hydroxyl group was demonstrated via mutagenesis studies. This is where; the Y7F mutant showed weakened activity and the Y7 hydroxyl group lowers the GSH sulfhydryl group pK_a. It is also through side directed mutagenesis that the significance of serine in S/C-type GST of human theta class was confirmed (Oakley, 2011).

2.9 Recombinant protein

Different levels of mRNA expression by RT-PCR for each isoform can be detected as GST expression is tissue specific with a varied distribution between tissues. In *Drosophila,* some GSTs also express in a tissue specific manner (Saisawang et al., 2012). According to the different functions, GST genes are expressed differently in tissues. Since the very beginning, GST activity and the transcriptional level have been used as biomarkers of contaminant in the aquatic species like marine mollusks. The measurement of the contaminant accumulation in the tissues provides information on how the contaminants influence the health of organisms biologically. A biomarker gene, mu GST gene, HdGSTM1, have been identified from the disk abalone (*Haliotis*

discus discus) cDNA library and by overexpressing it in *Escherichia coli* and the biochemical properties of recombinant GST and its inducible expression in the exposure of model endocrine-disrupting chemicals like PAH have been characterized. It was through the recombinant protein approach, it was found out that HdGSTM1 does not have proper catalytic structure, thus lacking enzymatic activities, but showed good inducibility with endocrine- disrupting chemicals hence suggesting its application as marine pollution biomarker (Wan et al., 2008).

Insect GST genes have been well characterized from a large number of insect species due to its GST activity association with insecticides resistance. At first, it was reported that the insect GST genes were intronless and rapidly expressed under stress. But this was later disagreed when more data was obtained showing the presence of 5' introns in the GST genes (Singh et al., 2007). As per the present investigation, every isoform of DmGST appears to be expressed in the late embryonic stages of *Drosophila melanogaster*. According to the *Drosophila* Genome Database, 12 out of the 41 transcripts are cell variants and 3 transcripts encode inactive enzymes. In all the 6 classes of GSTs, at least 1 or more genes generate alternative transcripts. This alternative splicing increases protein functional diversity and proteome complexity. Most of the recombinant DmGST isoforms were heterologously expressed in soluble forms, except for DmGSTD7 (truncated) and DmGSTE8 which were expressed as inclusion bodies (Saisawang et al., 2012). Sawicki et al., in order to study the delta classes of Drosophila genes, used PCR primers specific for the ten delta class genes to amplify the sequences from Drosophila genomic DNA and subcloned between the corresponding sites of pET-30a(+) into *E.coli* BL21(DE3)pLysS cells for expression of all proteins (Sawicki et al., 2003).

2.10 Protein purification

The combination of the proteomics methods creates a potential approach useful in isolating the GST and also identifying them. When it comes to GST protein purification, affinity chromatography is most widely used as generally the protein binds GSH affinity matrix. The targeted protein can be eluted from the matrix using the GSH buffer. Pal and group have reported that the usage of the affinity matrix revealed greatly complexed GST expression patterns, varying during development and between tissues. This is essential in the knowledge on complex continuum representing the GST proteome on the whole. Few of the matrixes used were GSTrap, glutathione-agarose and S-substituted glutathione (Pal et al., 2012). The glutathione conjugate of bromosulfophtalein (BSP) has also been used to trap GST proteins. But so far, only sigma and epsilon classes have been reported to be successfully being isolated using the BSP as a ligand (Alias and Clark, 2007). The eluted enzymes will be analyzed through the appearance of a discrete band pattern on SDS-PAGE which will denote a successful purification hence; the purified enzyme can be used for further studies to gain more information on the particular isoform (Ben-arie et al., 1993). According to Saisawang and group, only one third of the DmGSTs can be purified through the GSH affinity chromatography (GSTrap). Since none of the omega, theta and zeta class members could be purified using the conventional GST affinity chromatography hence it was suggested that it was necessary to develop purification protocols individually (Saisawang et al., 2012).

3.0 MATERIALS AND METHODS

3.1 Materials

Chemicals

- 0.5 M Tris-HCL pH 6.8 (BioRad, USA)
- 1.5 M Tris-HCL pH 8.8 (BioRad, USA)
- 30 % Acrylamide/bis-acrylamide (29:1) (Biorad, USA)
- Acetone (Sigma Aldrich, USA)
- Ammonium bicarbonate (Systerm)
- Ammonium persulphate (BioRad, USA)
- Ammonium sulpate (R&M Chemicals, UK)
- Benchmark Protein Ladder (Invitrogen, USA)
- Bovine Serum Albumin (Sigma Aldrich, USA)
- Cellytic B Buffer (Sigma Aldrich, USA)
- Chloroform (Systerm)
- Coomasie Brilliant Blue G-250 (Sigma Aldrich, USA)
- Ethanol (Systerm)
- Ethidium Bromide (Sigma Aldrich, USA)
- Gluthathione reduced (GSH) (Sigma Aldrich, USA)
- Isopropyl β-D-thiogalactopyranoside (IPTG) (Gold Bio.Com, USA)
- Methanol (Systerm)
- Nicotinamide Adenine Dinucleotide Phosphate (Sigma Aldrich, USA)
- Quercetin (Sigma Aldrich, USA)
- Sebacid acid (Sigma Aldrich, USA)
- Sodium Chloride (Systerm)
- Sodium dihydrogen phosphate (Systerm)

- Sodium Dodecyl Sulphate (Sigma Aldrich, USA)
- Sodium Hydroxide (Systerm)
- Tetradecanedioic acid (Sigma Aldrich, USA)
- Tetramethylethylenediamine (TEMED) (BioRad, USA)
- *trans*-Chalcone (Sigma Aldrich, USA)
- Triphenyltin acetate (Sigma Aldrich, USA)
- Triphenyltin hydroxide (Sigma Aldrich, USA)
- Tris Base (Promega,USA)

Kits

- pGEM-T Easy Vector Ligation Kit (Promega, USA)
- Genomic Extraction Kit (Qiagen, Germany)
- innuPREP Plasmid Rapid Kit (Analytik Jena, Germany)
- innuPREP DoublePure Rapid Kit (Analytik Jena, Germany)
- QuikChange Lightning Site-Directed Mutagenesis Kit (Agilent Technologies, USA)
- Clonables Kit (Novagen, USA)

Molecular Biology Consumables

- Accu Power PCR premix (Bioneer, Korea)
- EcoRI FastDigest restriction enzyme (Fermentas, USA)
- NdeI FastDigest restriction enzyme (Fermentas, USA)
- 1 kb DNA Ladder (Promega, USA)
- 6X Loading Dye (Fermentas, USA)
- Agarose LE Analytical grade (Promega, USA)
- pET-30a(+) plasmid DNA (Novagen, USA)

- *Escherichia coli* Competent Cell (BL21(DE3)pLysS) (Novagen, USA)
- NovaBlue Singles Competent Cells (Novagen, USA)
- Kanamycin sulphate (Calbiochem, Canada)
- Nuclease free water (Fermentas, USA)
- Luria Bertani Agar (Pronadisa)
- Luria Bertani Broth (Promega)

Substrates for Enzyme Assay

- 1,2-Dichloro-4-nitrobenzene (DCNB) (Sigma Aldrich, USA)
- 1-Chloro-2,4-dinitrobenzene (CDNB) (Sigma Aldrich, USA)
- *p*-Nitrophenyl Chloride (NBC) (Sigma Aldrich, USA)
- Ethacrynic acid (EA) (Sigma Aldrich, USA)
- Trans-4-phenyl-3-butene-2-one (PBO) (Sigma Aldrich, USA)
- Trans-2-octenal (Sigma Aldrich, USA)
- Trans-2-hexenal (Sigma Aldrich, USA)
- Hexa-2,4-dienal (Sigma Aldrich, USA)
- *trans,trans*-Hepta-2,4-dienal (Sigma Aldrich, USA)
- Cumene hyperoxide (Fluka, Sigma Aldrich, USA)
- Hydrogen peroxide (Sigma Aldrich, USA)

Buffer

- 10 X FastDigest Buffer 4 (Fermentas, USA)
- TBE Buffer (0.09 M Tris-Borate (BioRad, USA) and 2 mM EDTA (Sigma Aldrich, USA), pH 8.0)
- Buffer A (0.1 M Sodium Phosphate Buffer pH 6.8)
- Buffer B (0.1 M Tris Buffer pH 9.0)

- Buffer C (0.1 M Sodium Phosphate Buffer pH 7.5)
- Buffer D (0.25 M Sodium Phosphate Buffer pH 7.0)
- SDS reducing buffer [0.5 M Tris-HCl (BioRad, USA) pH 6.8, glycerol (Systerm), 10 % (w/v) SDS (Systerm) and 0.5 % (w/v) Bromophenol Blue (Sigma Aldrich, USA) and β mecapthoethanol (prior to use)]
- Tris/Glycine/SDS running buffer (25 mM tris, 192 mM Glycine and 0.1 % (w/v) SDS, pH 8.3) (BioRad, USA)

Instrumentation

- AKTA purifier FPLC (GE Healthcare, Sweden)
- Mycycler thermal cycler (Biorad, USA)
- Alpha Imager Mini Gel Documentation System (Protein Simple, USA)
- Centrifuger machine (Epperndorf, Germany)
- Microwave (Pensonic)
- Vortex mixer (Labnet International Inc, USA)
- WiseBath, Shaking incubator (Wisd Lab Equipments)
- Air clean PCR workstation (ISC Bioexpress)
- Orbital Shaker (Protech)
- Microprossecor pH211, pH metre (Hanna Instruments, USA)
- JASCO V630 spectrophotometer (JASCO, Japan)
- Mini-PROTEAN Electrophoresis with Bio-Rad power supply (Biorad, USA).
- Laminar hood (SASTEC)
- J-1500 High performance CD spectropolarimeter (JASCO, Japan)

3.2 Methods

3.2.1 Sample preparation

Drosophila melanogaster that were used in this study were obtained from the Genetics department of University Malaya (2011). Adult fruit flies were bred and maintained at room temperature on standard oats agar medium (Appendix 8.1). Newly emerged adult flies were continuously subcultured into new medium every week.

3.2.2 Total Genomic DNA extraction

The total genomic DNA was extracted from the adult fruitflies by using the Qiagen Genomic Extraction Kit. About 100 mg adult flies were homogenized during each extraction.

3.2.3 Cloning of recombinant gene

3.2.3.1 Polymerase chain reaction

Recombinant DNA techniques were performed using conventional methods. The total genomic DNA was used to amplify the target gene, DmGSTD3. The *gst* gene of *Drosophila melanogaster* was amplified using specific primers which produced a fragment of around 600 bp amplified DNA encoding the *gst* gene. Forward primers were designed to introduce an *NdeI* restriction site (underline) which includes the initiation codon ATG. Reverse primers spanned all or part of the stop codon (double underline) and were designed to introduce *EcoRI* restriction site (**boldface**)

Forward DmGSTD3: 5' –CGCTCCGTTCATATGGTGGGCAAG – 3'

Reverse DmGSTD3: 5' –TC**GAATTC**AATGAATTATTTAGCAGCATTCTG – 3'

Table 3.1: Formulation and thermal cycling protocol for Polymerase Chain Reaction of DmGSTD3

PCR Profile	Quantity
PCR premix-taq	10 µl
Forward primer	1 µl
Reverse primer	1 µl
Template DNA	X µl (5ng)
Sterile ddH_2O	X µl
Total	20 µl

Thermal cycling	Temperature (°C)	Duration	No. of Cycles
Pre-denaturation	95	3min	1
Denaturation	95	30sec	
Annealing	55	30sec	32
elongation	72	1min	

3.2.3.2 Gel electrophoresis

One g of agarose powder was dissolved in 100 ml of 0.5 X TBE buffer in order to prepare 1 % gel (w/v). The mixture was then briefly boiled in a microwave oven to completely dissolve. The flask containing the hot dissolved was left to cool under running tap water before pouring it slowly into the gel tray. Proper comb (1.5 mm) was inserted to form the well and the gel was left to harden for at least 30 minutes. Once harden, the gel was placed in the tank filled with 0.5 X TBE buffer and the comb was removed. 6 X loading dye were mixed with the DNA sample at a ratio of 1:5 and the mixture was loaded into the well with a pipette. One kb DNA ladder (Promega) was used as a standard marker. The loading dye colours the sample and provides density to the sample to move along the gel from negative to positive charge. Electrophoresis was performed at 60 V for approximately 1 hour and 30 minutes. Once the marker and

loading dye touches almost the bottom of the gel, the electrophoresis was stopped and the gel was removed from the tank to be placed in a container filled with diluted ethidium bromide (EtBr) solution (0.5 mg/ml) for 20 minutes. Then the gel is immersed in distilled water for about 10 minutes to destain the gel. The gel was then viewed under ultraviolet radiation (302 nm) to analyze the EtBr stained DNA bands.

3.2.3.3 Cloning into Amplification vector

The amplified DNA was the purified either by using a gel purification or PCR purification kit depending on the clarity of the PCR product on the agarose gel. The purified DNA was then ligated into the plasmid pGEM-T Easy through TA cloning using the T4 DNA ligase. The ligation reaction was then used to be transformed into NovaBlue Competent Cells (*Escherichia coli* JM109) on Luria-Bertani (LB) agar containing ampicilin (100 mg/ml) and IPTG-Xgal (Appendix 8.2). Through blue-white screening method, the transformants were chosen and, the pGEMT-D3 plasmid was extracted using innuPREP Plasmid Rapid Kit (Analytik Jena). The recombinant plasmid was further confirmed by restriction site analysis and was sequenced by BigDye Terminator v3.1 cycle sequencing kit chemistry using an ABI prism (FirstBase). The sequencing data was then analyzed using BLAST (Basic Local Alignment Search Tools) program through network services of the National Center for Biotechnology Information (http://www.ncbi.nlm.nih.gov).

Table 3.2: Ligation of the amplicon (DmGSTD3) and pGEM-T Easy Vector

Items	**TA Cloning (pGEM-T Easy)**
2X Rapid Ligation Buffer	5 µl
Insert	3 µl
Vector	1 µl
T4 DNA Ligase	1 µl
Sterile ddH_2O	-
Total	10 µl

The ligation reaction tubes were incubated at 16 °C for 16 hours.

3.2.3.4 Cloning into Expression Vector

The DNA encoding the GST gene was then subcloned into an expression vector pET-30a (+) in between NdeI and EcoRI sites. The digestion of DmGSTD3 amplicon and the vector (pET30a+) condition was tabulated in **Table 3.3**. While, the ligation conditions of the DNA fragments were tabulated in **Table 3.4**. The pET-D3 plasmid was then transformed into *E. coli* BL21 (DE3) pLysS strain on LB medium with kanamycin (30 mg/ml). All Glycerol stocks of the transformed cultures were kept in -80 ℃ freezer. To revive the stored culture, a tooth pick was used to scrap of the top layer of the frozen glycerol stock and inoculated into fresh LB medium or streaked on to LB plate medium and incubated at 37 ℃.

Table 3.3: Digestion of the amplicon (DmGSTD3) and vector (pET30a)

Items	**PCR product (Insert)**	**Plasmid (Vector)**
FastDigest 10X Buffer	3 µl	2 µl
PCR product (insert)	10 µl	-
Plasmid (vector)	-	2 µl
EcoR1	1 µl	1 µl
Nde1	1 µl	1 µl
Sterile ddH_2O	5 µl	4 µl
Total	30 µl	20 µl

The digestion reaction tubes were incubated at 37 ℃ for 2-16 hours.

Table 3.4: Ligation of the insert (DmGSTD3) and vector (pET-30a)

Items	**Sticky-end ligation (pET-30a)**
Clonable 2X Ligation Premix	5 µl
Insert	3 µl
Vector	1 µl
T4 DNA Ligase	-
Sterile ddH_2O	1 µl
Total	10 µl

The ligation reaction tubes were incubated at 16 ℃ for 16 hours.

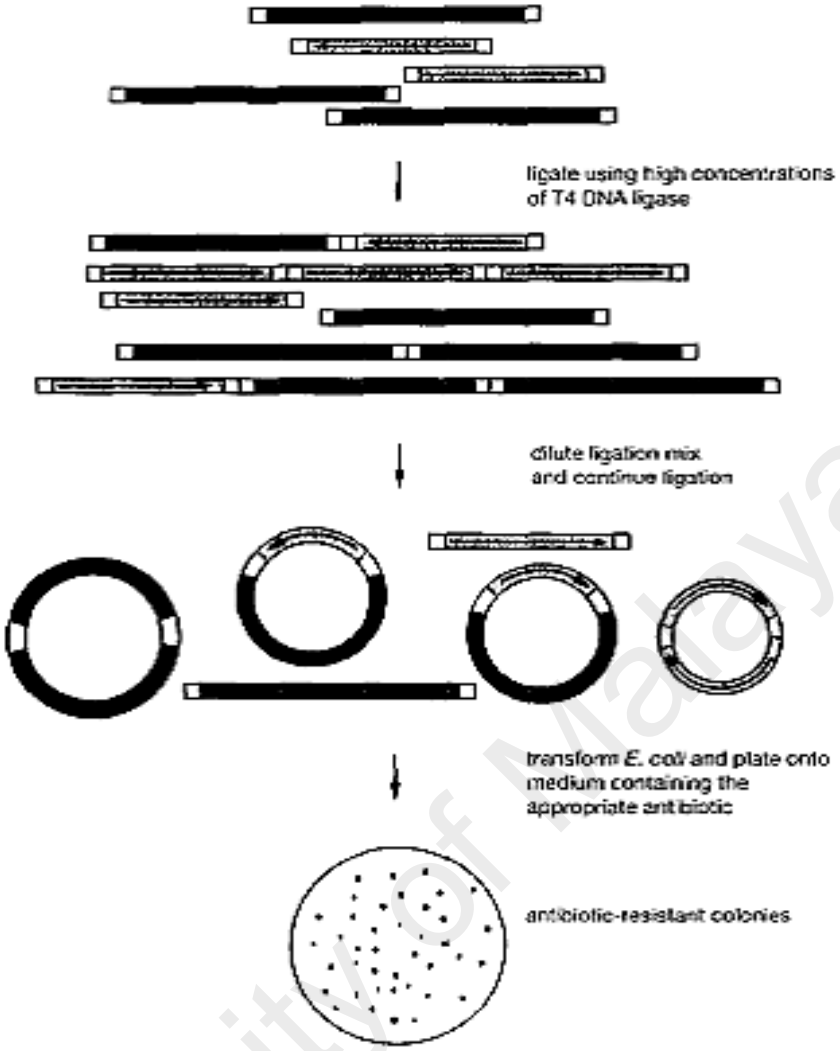

Figure 3.1 shows Blunt End Cloning Technique. Antibiotic resistant colonies arise due to the presence of the antibiotic resistant encoding gene that's present in the vector (Sambrook and Russell, 2001)

3.2.3.5 Side directed Mutagenesis

The QuikChange Lightning Site-Directed Mutagenesis Kit was used to make point mutations using the most advanced high fidelity enzyme technology. The simple, rapid three-step procedure requires only about one hour prior to transformation (for plasmids up to 5 kb), and generates mutants with greater than 85% efficiency in a single reaction (**Table 3.5**). The concept of the accelerated procedure is shown below.

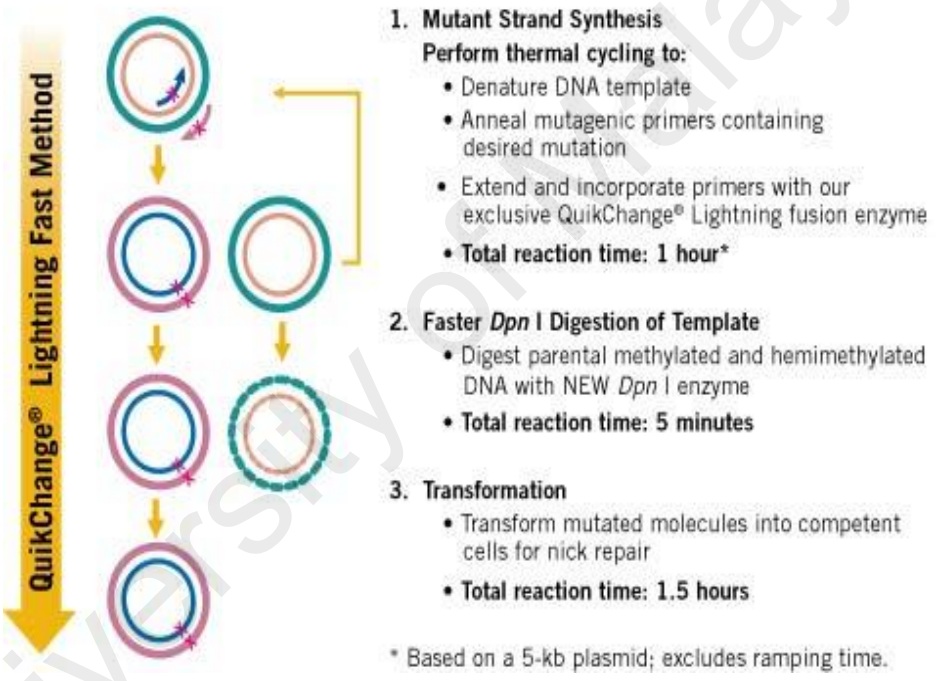

Figure 3.2 shows Overview of the QuikChange Lightning site-directed mutagenesis method (Agilent technologies instruction manual)

Two complimentary oligonucleotides primers containing the desired mutation, flanked by unmodified nucleotide sequence were synthesized according to the primer design guidelines from the manufacturer's manual. Bold alphabets represent the codons that codes for alanine instead of tyrosine.

Y89A	5'-tgatatggc**gc**tgatggctccgaccctggcgaac-3'
Y89A_antisense	5'-gttcgccagggtcgga**gc**catcagcgccatatca-3'
Y97A	5'-atccgaccctggcgaactattat**gc**taaagcgtttaccacc-3'
Y97A_antisense	5'-ggtggtaaacgctttta**gc**ataatagttcgccagggtcggat-3'

Table 3.5: Temperature cycling profile of side directed mutagenesis

Items	**Quantity**
10× reaction buffer	5 µl
dsDNA template	X µl (10 –100 ng)
oligonucleotide primer	X µl (125 ng)
oligonucleotide primer (antisense)	X µl (125 ng)
dNTP mix	1 µl
QuikSolution reagent	1.5 µl
ddH2O	to a final volume of 50 µl

Segment	**Cycles**	**Temperature**	**Time**
1	1	95	2 min
2	18	95	20 s
		60	10 s
		68	30 s/kb
3	1	68	5 min

3.2.3.6 Transformation Procedure

Competent cells were thawed on ice. Five µl of ligated DNA was added into the vial containing 50 µl competent cells and mixed by gentle taps (test plasmid for positive control and sterile distilled water for negative control). The cells were incubated in crushed ice for 30 minutes. The cells are then incubated at 42 ℃ for 30 seconds and immediately transferred into ice for another 2 minutes of incubation for heat-shock process. A total of 250 µl of pre-warmed SOC medium was then added into the vial. The vials were then secured in a rack with tape, and shaken for 1 hour at 37 ℃

at 225 rpm. Fifty µl of the transformed cells were then spread on Luria broth agar plates containing antibiotic. The plates were then incubated at 37 °C overnight.

3.2.4 Expression and purification of recombinant DmGSTD3

A single colony of transformed *E. coli* BL21 pET-D3 was inoculated into 5 ml LB medium containing kanamycin (30 µg/µl) and incubated on a shaking incubator at 37 °C for 16 hours. Then 500 µl of the overnight culture was diluted into a fresh 500 ml LB medium containing kanamycin. The culture was grown at 37 °C until optical density at 600 nm reached 0.6 (16-18 hours). The culture was then induced with 0.4 mM IPTG, and the incubation was continued for an additional 4 hours in the same condition. After incubation, the culture was then harvested by centrifugation at 6500 rpm for 20 minutes at 4 °C. The pelleted cells were resuspended in 2X Cellytic B buffer and mixed thoroughly with a vortex before incubating it on a shaker for 15 minutes. The lysate was then centrifuged at 10 000 rpm for 30 minutes at 4 °C to separate the cell debris. The clear supernatant was then separated and stored in 4 °C prior to purification and activity assay.

3.2.5 Purification using Fast Peptide Liquid Chromatography (FPLC)

The crude sample protein was loaded into the AKTA Purifier which was pre-equilibrated with sodium phosphate buffer (pH 7.4). The protein was purified using the 1ml GST-trap column (GE Healthcare). AKTA Purifier equipped with UNICORN software Version 3.2 and a fraction collector (Frac900) was employed for greater automation of the purification process. The sample was applied using a 5 ml syringe and the flow rate was fixed at 0.3 ml/min.

3.2.6 Affinity chromatography (GSTrap)

Once sample had been applied the pre-equilibrated column was washed with Sodium phosphate buffer, pH 8.0 to remove the unbound proteins. Subsequently, the recombinant proteins (GST) were eluted with freshly prepared 10 mM GSH elution buffer (pH 8.0). Following the chromatography the collected fractions were pooled according to the absorbance peak. The collected fractions were then measure for activity and the active fractions were pooled and saved for further analysis.

a) Preparation of Running buffer, 25 mM Sodium Phosphate Buffer, pH 8.0:

   3 g of NaH_2PO_4 was dissolved in 900 ml of distilled water. The pH of the solution was adjusted to 7.35 at 20 °C and the volume was made up to 1000 ml.

b) Preparation of Elution buffer, 10 mM GSH buffer, pH 8.0:

   0.307 g of GSH was dissolved in 90 ml of Sodium Phosphate Buffer. The pH of the solution was adjusted to 7.35 and the volume was made up to 100 ml

3.2.6.1 Anion Exchange (Q-HP, 5 ml) (GE Healthcare)

Once sample had been applied the pre-equilibrated Q-HP column was washed with Sodium phosphate buffer, pH 8.0 to remove the unbound proteins. Subsequently, the recombinant proteins (GST) were eluted with 0.5 M Sodium chloride elution buffer (pH 8.0). Following the chromatography the collected fractions were pooled according to the absorbance peak. The collected fractions were then measure for activity and the active fractions were pooled and saved for further analysis.

3.2.7 SDS-Polyacrylamide Gel (PAGE)

The purity of the concentrated protein was confirmed using the SDS PAGE. SDS PAGE analysis was performed using Mini-PROTEAN Electrophoresis units with a Bio-Rad power supply (Biorad Laboratories, USA). The polyacrylamide gels were prepared according to below formulation. All gel casting material were washed with distilled water and wiped clean with acetone. The resolving part was prepared first and overlaid with distilled water to be allowed to polymerize for an hour or more. Once harden, the overlaid distilled water is poured away and replaced with the stacking gel. Both the gel solution were degas before adding the tetramethylethylenediamine (TEMED) and ammonium persulphate (APS). A comb was placed above the stacking gel immediately after the gel is poured to allow well formation.

Table 3.6: SDS PAGE gel casting (**Appendix 8.3**)

SDS PAGE Gel Formulation	**Stacking Gel (4%)**	**Resolving Gel (12%)**
Deionised water	15	3.4
30% (w/v) Acrylamide/bis-acrylamide	3.3	4.0
1.5 M Tris-HCl (pH8.8)	-	2.5
0.5 M Tris-HCl (pH6.8)	6.3	-
10% (w/v) SDS	0.25	0.1
10% (w/v)APS	25.0 µl	25.0 µl
TEMED	0.005	0.005

The electrophoresis apparatus were assembled following the manufacturer's instructions for Bio-Rad Mini-PROTEAN II System. The protein samples were diluted with SDS sample buffer (**Appendix 8.3**) at a ratio of 1:2 and heated at 95 °C for 4-5 minutes prior to loading into the gel wells along with a protein standard marker. Electrophoresis was carried out at 120 V for 1 hour with running buffer 1X Tris-glycine buffer (25 mM Tris-HCl pH 8.6, 192 mM Glycine and 0.1 % SDS). For protein

visualization, the gels were stained with Coomasie staining solution overnight and destained with 20 % methanol. The gel was viewed under visible white light.

3.2.7.1 Colloidal Coomassie Brilliant Blue G-250.

One g of Coomassie Brilliant Blue G-250 was added in 20 ml of dH_2O and sonicated until it dissolved. A total of 11.8 ml of 85 % phosphoric acid is added to the CBB solution. 100 g of ammonium sulphate was dissolved in approximately 600 ml of dH_2O. Then the CBB solution was added little by little and made up to 1 L.

3.2.8 Protein Quantification (Bradford Assay)

A total of 100mg Coomasie Brilliant Blue G-250 was dissolved in 50 ml 95 % (v/v) ethanol and 100 ml of 85 % (w/v) phosphoric acid was added to the mixture. The solution was then diluted to 1 litre once the dye had been fully dissolved, and was filtered through Whatman #1 paper just before used. The filtered Bradford solution was poured into a flask and wrapped in aluminum foil, stored in dark place.

Standard, bovine serum albumin (BSA) ranging from 20-100 µg was prepared in 100 µl volume. Five ml Bradford reagent was added and mixed well with a vortex mixer. Mixture was then incubated for 5 minutes in dark. Absorbance measured at 595 nm (Bradford, 1976).

3.2.9 Enzymatic Assays

Conjugation of common GST substrates was performed according to Habig et al., (1974) and Brophy et al., (1989).

3.2.9.1 1-Chloro-2,4-dinitrobenzene (CDNB)

All the below was added in a cuvette accordingly and mixed well:

2.85 ml Buffer A

0.05 ml 60 mM GSH (freshly prepared)

0.05 ml sample

0.05 ml of 60 mM CDNB

The sample was replaced with potassium phosphate buffer for negative control. Enzyme activity conjugating GSH to the CDNB was measured by monitoring the increasing in absorbance at 340 nm over time using JASCO V360 spectrophotometer. This standard GST assay was performed at 25 °C and monitored for 10 minutes. Molar absorption coefficient ξm, is 9600 $Lmol^{-1}cm^{-1}$ (Habig et al., 1974).

3.2.9.2 1,2-Dichloro-4-nitrobenzene (DCNB)

All the below was added in a cuvette accordingly and mixed well:

2.80 ml Buffer B

0.05 ml 240 mM GSH (freshly prepared)

0.10 ml sample

0.05 ml of 24 mM DCNB

The sample was replaced with potassium phosphate buffer for negative control. Enzyme activity conjugating GSH to the DCNB was measured by monitoring the increasing in absorbance at 344nm over time using JASCO V360 spectrophotometer. This standard GST assay was performed at 25 °C and monitored for 20 minutes. Molar absorption coefficient ξm, is 8400 $Lmol^{-1}cm^{-1}$ (Motoyama and Dauterman, 1974).

3.2.9.3 *p*-Nitrophenyl Chloride (NBC)

All the below was added in a quartz cuvette accordingly and mixed well:

2.60 ml Buffer A

0.25 ml 60 mM GSH (freshly prepared)

0.10 ml sample

0.05 ml of 60 mM NBC

The sample was replaced with potassium phosphate buffer for negative control. Enzyme activity conjugating GSH to the NBC was measured by monitoring the increasing in absorbance at 310nm over time using JASCO V360 spectrophotometer. This standard GST assay was performed at 25 °C and monitored for 10 minutes. Molar absorption coefficient ξm, is 1900 $Lmol^{-1}cm^{-1}$ (Habig et al., 1974).

3.2.9.4 *trans*-2-octenal

All the below was added in a quartz cuvette accordingly and mixed well:

2.85 ml Buffer A

0.05 ml 60 mM GSH (freshly prepared)

0.05 ml sample

0.05 ml of 60 mM *trans*-2-octenal

The sample was replaced with potassium phosphate buffer for negative control. Enzyme activity conjugating GSH to the *trans*-2-octenal was measured by monitoring the increasing in absorbance at 225 nm over time using JASCO V360 spectrophotometer. This standard GST assay was performed at 25 °C and monitored for 10 minutes. Molar absorption coefficient ξm, is -22000 $Lmol^{-1}cm^{-1}$ (Habig et al., 1974).

3.2.9.5 *trans*-2-hexanal

All the below was added in a quartz cuvette accordingly and mixed well:

2.85 ml Buffer A

0.05 ml 60mM GSH (freshly prepared)

0.05 ml sample

0.05 ml of 60 mM *trans*-2-hexanal

The sample was replaced with potassium phosphate buffer for negative control. Enzyme activity conjugating GSH to the *trans*-2-hexanal was measured by monitoring the increasing in absorbance at 225 nm over time using JASCO V360 spectrophotometer. This standard GST assay was performed at 25 °C and monitored for 10 minutes. Molar absorption coefficient ξm, is -22000 $Lmol^{-1}cm^{-1}$ (Habig et al., 1974).

3.2.9.6 Ethacrynic acid (EA)

All the below was added in a cuvette accordingly and mixed well:

2.80 ml Buffer A

0.05 ml 15 mM GSH (freshly prepared)

0.10 ml sample

0.05 ml of 12 mM EA

The sample was replaced with potassium phosphate buffer for negative control. Enzyme activity conjugating GSH to the EA was measured by monitoring the increasing in absorbance at 270 nm over time using JASCO V360 spectrophotometer. This standard GST assay was performed at 25 °C and monitored for 10 minutes. Molar absorption coefficient ξm, is 5000 $Lmol^{-1}cm^{-1}$ (Habig et al., 1974).

3.2.9.7 Trans-4-phenyl-3-butene-2-one (PBO)

All the below was added in a cuvette accordingly and mixed well:

2.80 ml Buffer A

0.05 ml 15 mM GSH (freshly prepared)

0.10 ml sample

0.05 ml of 3 mM PBO

The sample was replaced with potassium phosphate buffer for negative control. Enzyme activity conjugating GSH to the PBO was measured by monitoring the increasing in absorbance at 290 nm over time using JASCO V360 spectrophotometer. This standard GST assay was performed at 25 °C and monitored for 10 minutes. Molar absorption coefficient ξm, is -24800 $Lmol^{-1}cm^{-1}$ (Habig et al., 1974).

3.2.9.8 Hexa-2,4-dienal

All the below was added in a cuvette accordingly and mixed well:

2.80 ml Buffer A

0.05 ml 150 mM GSH (freshly prepared)

0.10 ml sample

0.05 ml of 3 mM Hexa-2,4-dienal

The sample was replaced with potassium phosphate buffer for negative control. Enzyme activity conjugating GSH to the Hexa-2,4-dienal was measured by monitoring the increasing in absorbance at 280 nm over time using JASCO V360 spectrophotometer. This standard GST assay was performed at 25 °C and monitored for 10 minutes. Molar absorption coefficient ξm, is -34200 $Lmol^{-1}cm^{-1}$ (Brophy et al., 1989).

3.2.9.9 *trans,trans*-Hepta-2,4-dienal

All the below was added in a cuvette accordingly and mixed well:

2.80 ml Buffer A

0.05 ml 150mM GSH (freshly prepared)

0.10 ml sample

0.05 ml of 3 mM *trans,trans*-Hepta-2,4-dienal

The sample was replaced with potassium phosphate buffer for negative control. Enzyme activity conjugating GSH to the *trans,trans*-Hepta-2,4-dienal was measured by monitoring the increasing in absorbance at 280 nm over time using JASCO V360 spectrophotometer. This standard GST assay was performed at 25 °C and monitored for 10 minutes. Molar absorption coefficient ξm, is -30300 $Lmol^{-1}cm^{-1}$ (Brophy et al., 1989).

3.2.9.10 Cumene hyperoxide/ Hydrogen peroxide

All the below was added in a cuvette accordingly and mixed well:

2.70 ml Buffer D

0.05 ml 10 mM GSH (freshly prepared)

0.05 ml Glutathione reductase

0.05 ml 3.5 mM NADPH

0.10 ml sample

0.05 ml of 3 mM ROOH (hydrogen peroxide, cumene hydroperoxide)

The sample was replaced with potassium phosphate buffer for negative control. Enzyme activity conjugating GSH to the hydrogen peroxide was measured by monitoring the increasing in absorbance at 366 nm over time using JASCO V360 spectrophotometer. This standard GST assay was performed at 25 °C and monitored for 20 minutes. Molar absorption coefficient of NADPH, ξm, is 6220 $Lmol^{-1}cm^{-1}$ (Wendel, 1981).

3.2.10 GST Sequence search and analysis

Similarity and sequence comparing was one of the approaches used from the available databases. One of the tools used was BLAST (Basic Local Alignment Search Tool), which performs comparisons between pairs of sequences, searching for regions of local similarity. BLAST was accessed from National Centre for Biotechnology Information (NCBI) (http://www.ncbi.nlm.nih.gov/) similarity with the native GST-D3 of the *Drosophila melanogaster*. Then the protein information was obtained from FlyBase (http://flybase.org/) which is a comprehensive database for information on genetics and molecular biology of Drosophila. The tertiary structure of the protein was searched from UniProt database (http://www.uniprot.org/) which consists of SWISS-PROT and downloaded from SWISSMODEL (http://swissmodel.expasy.org/).

Sequence alignment was performed using CLUSTALW programs (BioEdit) with default parameterization.

3.2.11 Inhibition Assay for IC_{50} determination

Inhibitors available (Triphenyltin hydroxide, Quercetin, *trans*-Chalcone, Tetradecanedioic acid, Sebacid acid and Triphenyltin acetate) was added at different concentrations into the reaction mixture containing 1 mg/ml GSTD3 and 1 mM of reduced glutathione (GSH) in buffer A. The assay condition includes:

Blank: 3.0 mL of buffer A

Control: 2.85 ml Buffer A

0.05 ml 60 mM GSH (freshly prepared)

0.05 ml inhibitor

0.05 ml of 60 mM CDNB

Sample: 2.80 ml Buffer A

0.05 ml 60 mM GSH (freshly prepared)

X ml inhibitor (0.2-1.4 mM)

0.05 ml 1 mg/ml GSTD3 (freeze-dried)

0.05 ml of 60 mM CDNB

The volume of inhibitor (stock: 1 mM, diluted in ethanol) was added according to the molarity needed for the study and additional Buffer A was used to top up the total volume of the reaction to 3 ml. Enzyme activity conjugating GSH to the CDNB with different concentration of inhibitor was measured by monitoring the increasing in absorbance at 340 nm over time using JASCO V360 spectrophotometer. This standard

GST assay was performed at 25 °C and monitored for 10 minutes. Molar absorption coefficient ξm, is 9600 $1.mol^{-1}cm^{-1}$ (Habig et al., 1974).

The percentage inhibition on GST-P activity (%) by each sample was calculated as following;

Percentage of inhibition, % =

$$\frac{(A_{sample} - A_{blank}) - (A_{control} - A_{blank})}{(A_{control} - A_{blank})} \text{ X } 100\%$$

Where, A represents the difference of the absorbance in the reaction with inhibitors overtime, of sample, blank and control respectively. The IC_{50} value indicates the concentration of the inhibitor at which the GSTD3 activity was inhibited by 50 %. The IC_{50} value was determined from the graph of percentage of inhibition on GST activity (%) versus concentration of inhibitor, generated using the software Microsoft Excel.

3.2.12 Kinetic characterization

The kinetic characterization of GSTD3 wildtype and mutant towards two variables, GSH and CDNB was studied independently in order to further understand the role of the mutations. During each activity assay, one of the substrate concentrations was maintained at 1 mM while the concentration of another was varied from 0.2 mM till 1.0 mM to study on the kinetic characteristics of the GSTD3 (wildtype/mutants) towards substrate with varying concentration. The concentration of protein sample was kept constant 1mg/ml during each reaction. Changes in activity were monitored at the wavelength of 340 nm at 25 °C for 10 minutes using JASCO V630 spectrophotometer.

Spontaneous reaction between GSH and CDNB in the absence of GSTD3 was corrected from the Control reading. V_{max} and K_m values of GSTD3 with varying CDNB or GSH concentration were generated using SigmaPlot 12.0 graph and analysis software.

3.2.13 Effect of temperature on GSTD3 activity

The effect of the temperature in the enzyme GSTD3 catalytic activity was studied by manipulating the temperature condition during the GSTD3 activity assay towards CDNB. The range of temperature studied was in between 15 °C to 42 °C. The assay was carried out exactly according to **3.2.9.1** but the temperature of the thermomixer was adjusted to 15 °C, 25 °C, 37 °C and 42 °C accordingly. The buffer with protein sample was incubated in the thermomixer for 15 minutes at the appropriate temperature prior to adding the GSH and CDNB. Enzyme activity conjugating GSH to the CDNB was measured by monitoring the increasing in absorbance at 340 nm over time using JASCO V360 spectrophotometer. This standard GST assay was performed at different temperatures and monitored for 10 minutes. Molar absorption coefficient ξm, is 9600 $Lmol^{-1}cm^{-1}$ (Habig et al., 1974). Then a graph of enzyme rate against different temperature was plotted. Base on the curve, the temperature at where GSTD3 protein activity is the highest rate was determined.

3.2.14 Effect of pH on GSTD3 activity

The effect of the pH on the enzyme GSTD3 stability was studied by manipulating the pH condition during the GSTD3 activity assay towards CDNB. The range of pH studied was in between pH 3 to pH 10. The assay was carried out exactly

according to **3.2.9.1** but the Buffer A was replaced with different ranged pH buffers. The assay for pH 3 to pH 6 was performed with Citrate phosphate buffer, pH 6.2 to pH 7.8 with sodium phosphate buffer and pH 8 to pH 10 with tris-HCl buffer. Enzyme activity conjugating GSH to the CDNB was measured by monitoring the increasing in absorbance at 340 nm over time using JASCO V360 spectrophotometer. This standard assay was performed at 25 °C and monitored for 10 minutes. Molar absorption coefficient ξm, is 9600 $Lmol^{-1}cm^{-1}$ (Habig et al., 1974). Then a graph of enzyme rate against different pH was plotted. Base on the curve, the pH at where GSTD3 protein activity is the highest rate was determined.

3.2.15 Circular Dichroism (CD)

High performance CD spectropolarimeter (JASCO) was used to measure the CD value of wildtype and mutant proteins to look into their secondary folding structure. The machine was connected to a thermal controller and a nitrogen supplier. A quartz cuvette (0.1 mm) was used to load our diluted protein sample (0.2 mg/ml). The structure of the protein sample, i.e alpha helix and beta sheet content was analyzed by looking at the CD spectrum. The modulation method was used to measure the CD effect in the spectrometer. The plane polarized light is split into the L and R components by passage through a modulator subjected to electric fields (Kelly et al., 2005).

4.0 RESULTS

4.1 Total Genomic DNA extraction

In order to study the DmGSTD3, the total genomic DNA was extracted to facilitate the gene amplification and further gene studies. Absorbance was read at 260 nm and 280 nm to evaluate the purity of the extracted genome. The ratio of absorbance (260 nm : 280 nm) in the range of 1.7 to 2.0 indicated high purity of DNA extraction. The size of the total genomic DNA has been reported to be 179 Mbp (Dimitri, 2002). Below is the image of the genomic DNA that was extracted using the Qiagen Genomic Extraction Kit on a 1% (w/v) agarose gel.

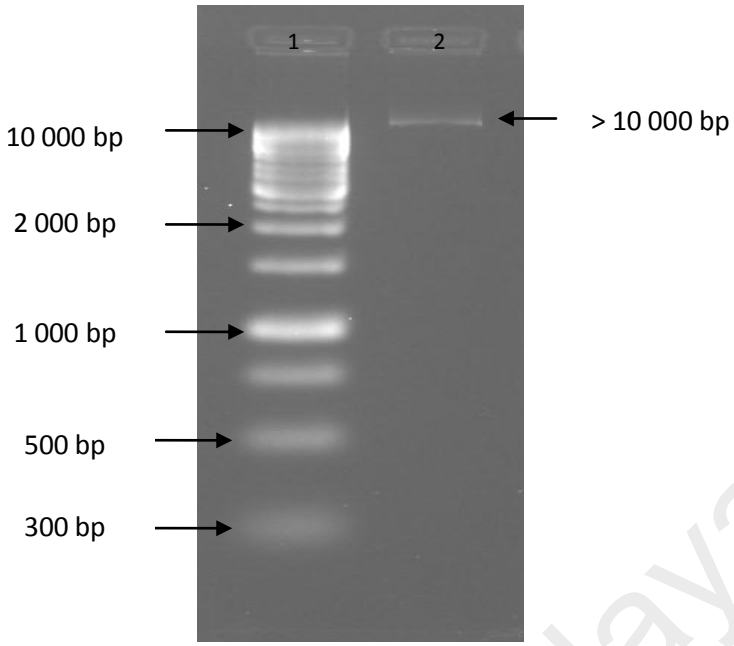

Figure 4.1 shows gel electrophoresis image of *Drosophila melanogaster* Genomic DNA extraction. Arrow at Lane 2 indicates the 2 ul of genomic DNA loaded onto 1% (w/v) agarose gel.
Lane 1: 1 kb DNA Ladder
Lane 2: Genomic DNA of *D. melanogaster*

4.2 Cloning of recombinant gene

4.2.1 Polymerase Chain reaction

Referring to Sawicki et al. (2003), forward primers were designed to introduce an *Nde*I restriction site (underline) which includes the initiation codon ATG. Reverse primers spanned all or part of the stop codon (double underline) and were designed to introduce *EcoR*I restriction site (**boldface**)

Forward DmGSTD3 5' -CGCTCCGTTCATATGGTGGGCAAG

Reverse DmGSTD3 5' –TC**GAATTC**AATGAATTATTTAGCAGCATTCTG

The annealing temperature was optimized at 55 °C since it gave the best single band of PCR product during PCR optimization.

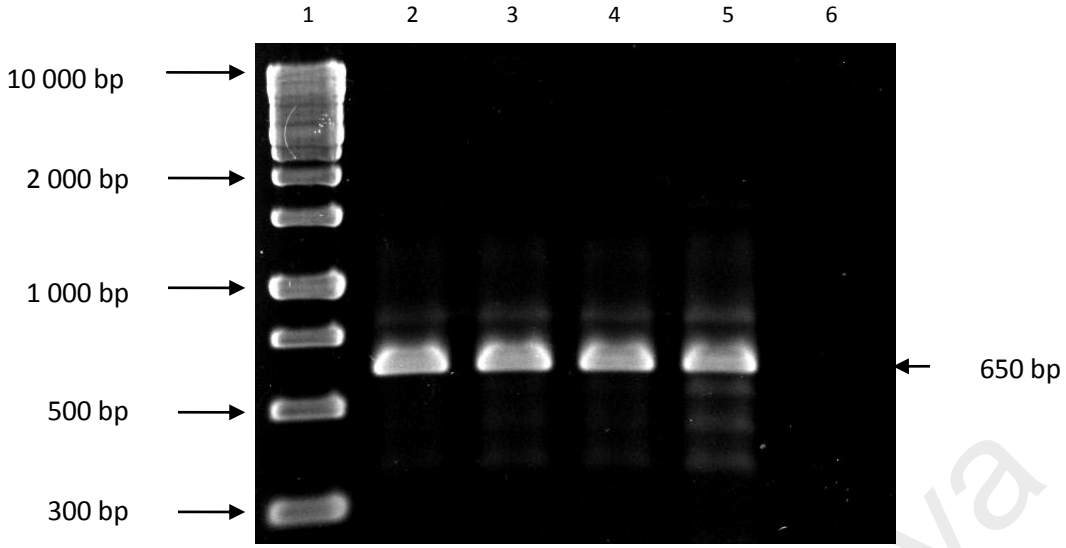

Figure 4.2 shows a gel electrophoresis image of PCR product of different annealing temperatures. Arrow indicates the PCR product of DmGSTD3 gene on a 1.0 % (w/v) agarose gel at above 650 bp.

Lane 1: 1 kb Marker
Lane 2: PCR with 55 °C annealing temperature
Lane 3: PCR with 57 °C annealing temperature
Lane 4: PCR with 59 °C annealing temperature
Lane 5: PCR with 62 °C annealing temperature
Lane 6: Negative Control (sterile distilled water)

4.2.2 pGEMT-D3 clone construction

In pGEMT-Easy cloning, generally white colonies contain inserts; therefore only white colonies were picked and cultured. Through observation (**Figure 4.3)**, the ratio of white and blue colonies on the transformation plate was 1:1. Then the plasmids were extracted from the culture and the gel electrophoresis was performed to confirm the right size of the recombinants. This was further verified by PCR using the pGEMT-D3 as template DNA. An amplified DNA band was observed at about 690 bp as seen in **Figure 4.4**. Once the recombinant pGEMT-D3 plasmids were obtained, 30 % (w/v) glycerol stocks were prepared where; 700 µl of overnight culture of a single colony was mixed with 300 µl of sterile glycerol. These were then labeled and stored in the -80 °C freezer.

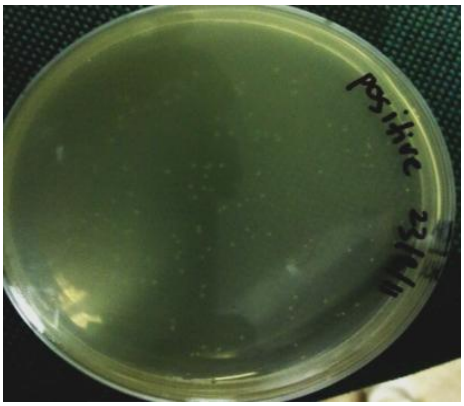

4.3a

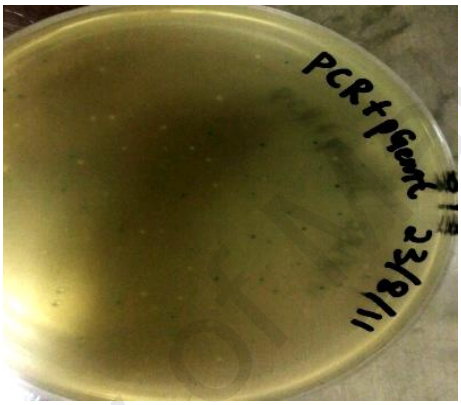

4.3b

4.3c

Figure 4.3 shows the transformant plates of pGEMT Easy vector with DmGSTD3 gene in *Escherichia coli* JM109 on AIX-LB plate (ampicilin-IPTG-Xgal). 4.3a shows positive control; 4.3b shows transformation colonies and 4.3c shows negative control (sterile distilled water)

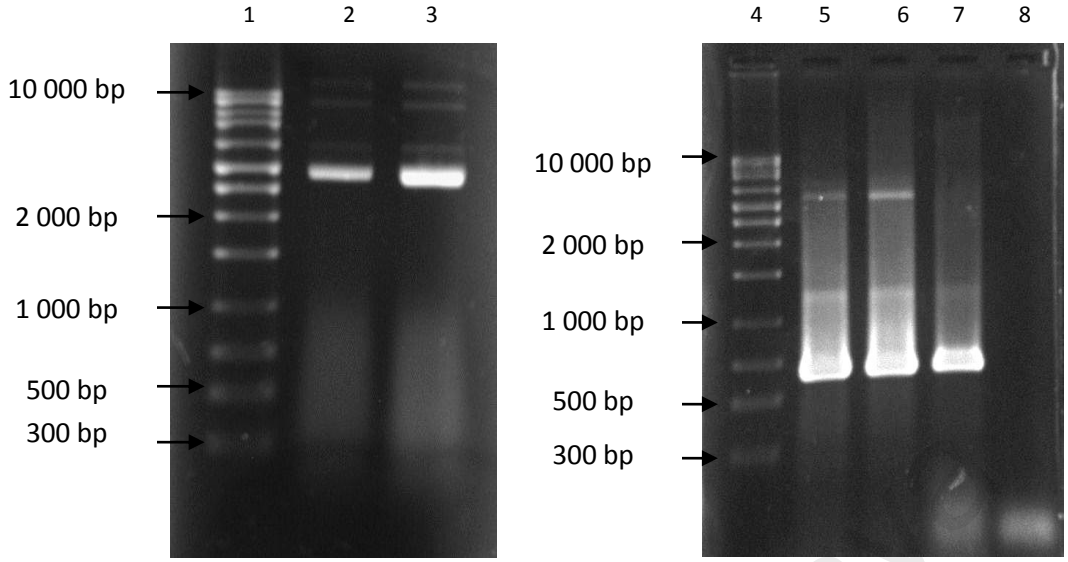

Plasmid extraction Insert Verification (PCR)

Figure 4.4 shows the gel image of recombinant plasmid of pGEMT-D3. Arrows indicate the plasmid extracted from *Escherichia coli* JM109 above 3000 bp and the PCR product representing the insert gene (DmGSTD3) at above 690 bp respectively.

Lane 1: 1 kb Marker
Lane 2: pGEMT-D3 (colony 1)
Lane 3: pGEMT-D3 (colony 2)
Lane 4: 1 kb Marker
Lane 5: PCR with DmGSTD3 primers (colony 1)
Lane 6: PCR with DmGSTD3 primers (colony 2)
Lane 7: Positive control (total genome)
Lane 8: Negative control (sterile distilled water)

4.2.3 pET30a-D3 clone construction

The gene of interest, i.e, DmGSTD3 was excised from the pGEMT-D3 plasmids and cloned into the pET-30a vector in between *Nde*1 and *EcoR*1 restriction sites. The ligated vector was then transformed into the *E. coli* BL21 (DE3) pLysS host to be expressed. A negative control was also done by replacing the ligated product with sterile distilled water. The plasmid were then extracted from the transformants and sent for sequencing.

4.3 GST Sequence search and analysis

4.3.1 Sequencing results

The nucleotide obtained from the sequencing results was then aligned with the GST reference sequence (NM 176479.2) from the NCBI database (http://www.ncbi.nlm.ni h.gov/nuccore/NM 176479.2). **Figure 4.6** is the sequence alignment results of the DmGSTD3 amino acids sequence and the reference amino acids sequence using the CLUSTALW software. As shown in **Figure 4.5**, the query sequence had 100 % similarity with the reference sequence, NM 176479.2 in BLAST. This proves that the recombinant gene clones has no mutations. Hence, further studies can be done on the recombinant plasmid.

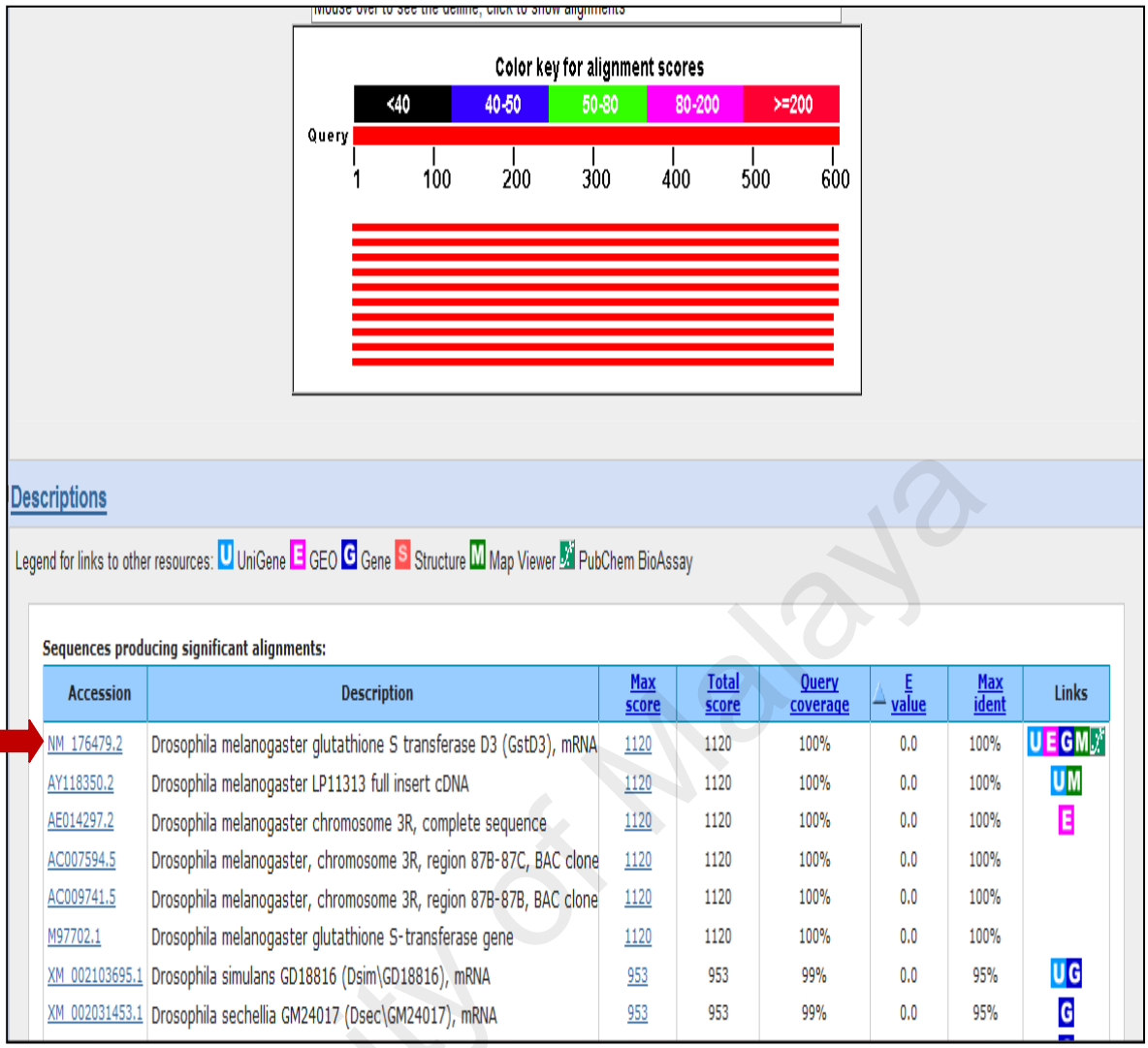

Figure 4.5 shows the print-screened BLAST search tool result on the recombinant gene of DmGSTD3 in pET-30a. The nucleotide sequence has 100 % identity with *Drosophila melanogaster* glutathione S transferase D3, mRNA (NM 176479.2).

4.3.2 Sequence alignment between different delta classes of the *Drosophila melanogaster*

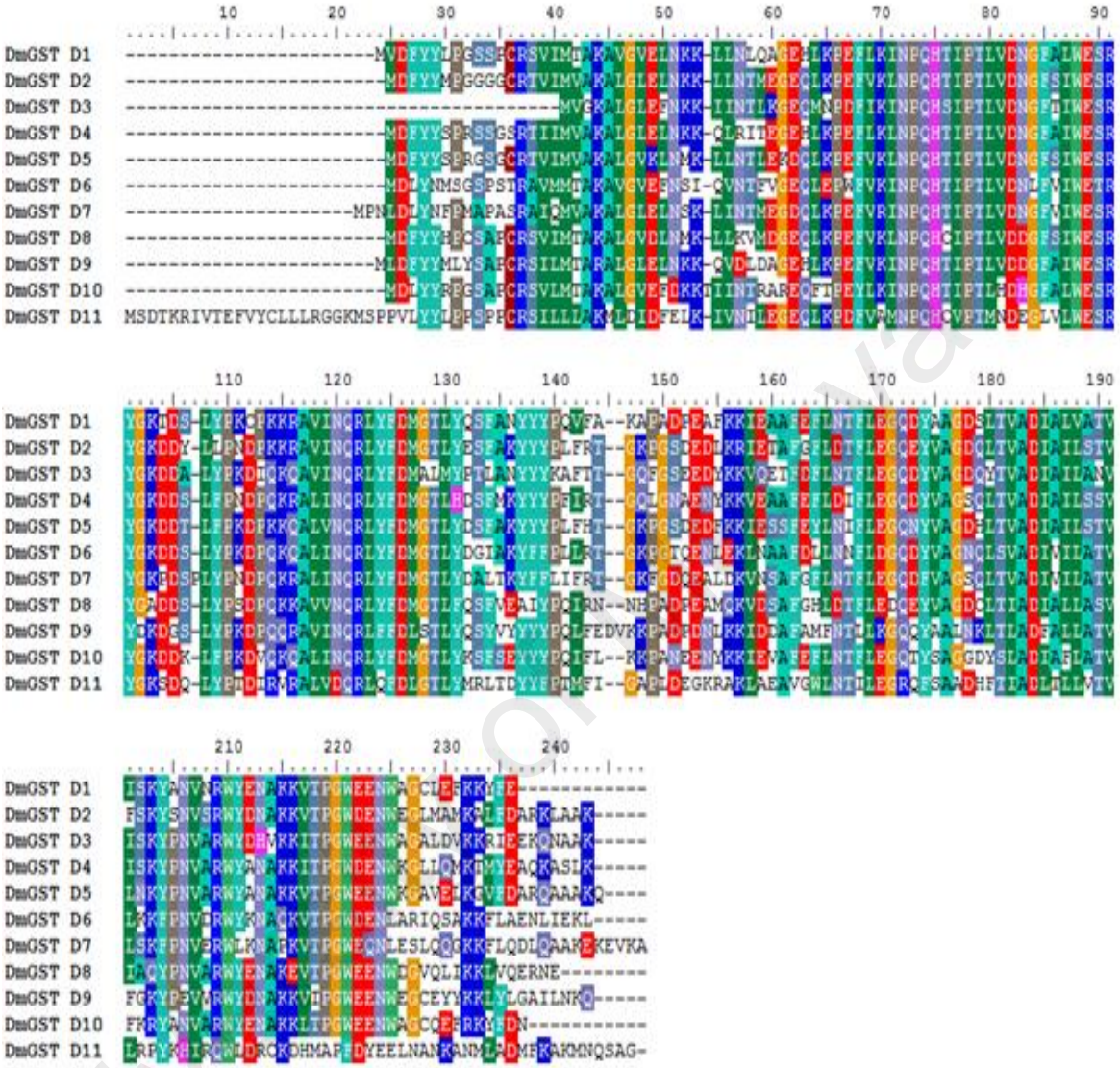

Figure 4.6 shows the alignment of all delta class GST amino acid sequences of *Drosophila melanogaster*. The missing 11 amino acids from the N-terminal proves the truncation and the lost of conserved tyrosine region. Multiple sequence alignment was done using ClustalW from BioEdit version 7.0.9.0 (Bioedit Seq Alignment Editor).

4.4 Structural studies

Homology studies were done on the GSTD3 structure to find out the potential amino acids at the GSH binding cavity side for further studies. The structure in **Figure 4.7** is the 3D model of GSTD3 with GSH binding to its catalytic side was obtained from the SWISS MODEL Repository (Uniprot: Q9VG97). The structure was viewed using the Swiss-PdbViewer 4.1.0. Through the tertiary structure it can be seen that two tyrosines at the position of 89 and 97 were pointing right into the catalytic cavity. The force field energy of both the tyrosines was calculated in **Table 4.1** using the GROMOS96 in order to observe its potential as the residues being involved in the GSH conjugation.

Table 4.1: Force field energy of Tyr89 and Tyr97 deduced with GROMOS96 in SwissPDB viewer.

	Bonds	**Angles**	**Torsion**	**Total**
Tyr89	1.364	15.290	6.315	22.969
Tyr97	0.630	16.566	4.056	21.252

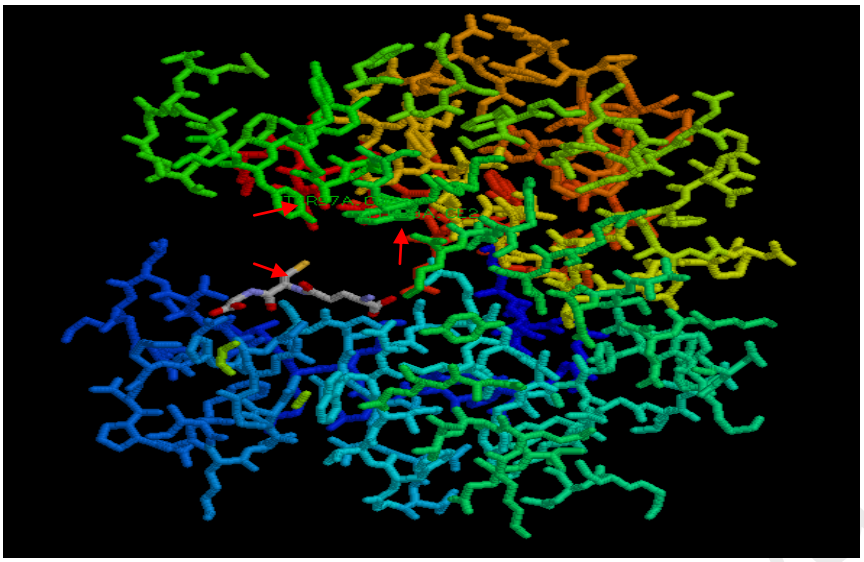

A

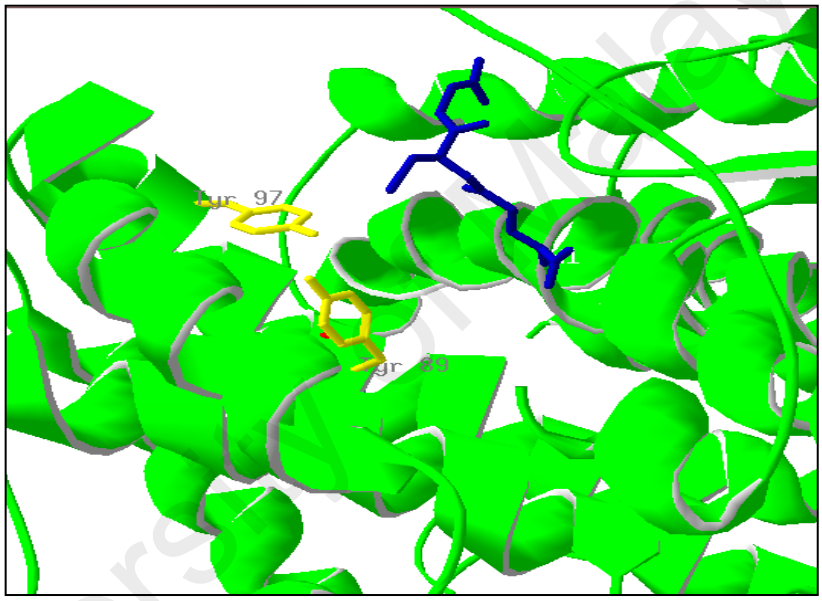

B

Figure 4.7 (A) shows the 3D model of the GSTD3 structure with the ligand (GSH) bound at the catalytic region viewed using the RasMol 2.7.5.2; **(B)** shows the position of the targeted tyrosines (Yellow) at 89 and 97 with the GSH (Blue) bound to the protein viewed using the Swiss-PdbViewer 4.1.0.

4.5 Expression and purification of recombinant DmGSTD3

GSTD3 was purified using a simple procedure which involved a QHP ion exchange column fixed to the FPLC system. Gradient elution was performed in order to identify the NaCl concentration that gives the most purified fraction. The 0.5 M NaCl elution gave the most purified band as observed on SDS PAGE and a relatively high activity. The pH of the purification was fixed to pH 8.0 as any pH lower than that result in some GSTD3 protein to be present in the void flow through. This optimized purification method was the fixed for further purifications GSTD3 wildtype and mutants proteins in mass quantity, which were all freeze-dried later for storage and bioassays.

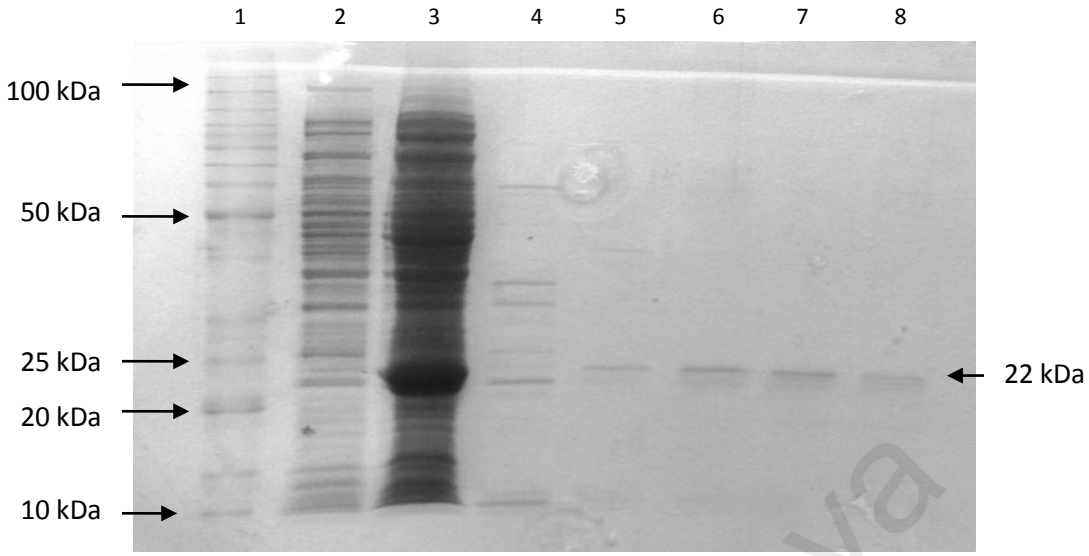

Figure 4.8 shows the SDS PAGE of crude protein extracted from the *E. coli* BL21and also the unbound and bound proteins during the purification of GSTD3 using QHP column. The gel was stained using the colloidal coomasie blue staining method. Arrow indicated the GSTD3 expressed at about 22 kDa.

Lane 1: 1 kb BenchMark Biorad
Lane 2: Crude lysate of control *E. coli* BL21
Lane 3: Crude lysate of cloned *E. coli* BL21 DmGSTD3
Lane 4: Unbound proteins of cloned *E. coli* BL21 crude
Lane 5: Eluted protein with 0.25 M NaCl, pH 8.0
Lane 6: Eluted protein with 0.50 M NaCl, pH 8.0
Lane 7: Eluted protein with 0.75 M NaCl, pH 8.0
Lane 8: Eluted protein with 1.0 M NaCl, pH 8.0

4.6 Enzymatic Assays

4.6.1 Substrates specificity

Table 4.2 shows the different substrates used to check the substrates specificity of GSTD3. Based on the results, CDNB was the only substrate to have activity with the enzyme with a specific activity of 7.38 μmol/min/mg.

Table 4.2: Substrates specificity of GSTD3

Substrates	Specific activity (μmol/min/mg)
1-Chloro-2,4-dinitrobenzene (CDNB)	7.38 ± 0.42
1,2-Dichloro-4-nitrobenzene (DCNB)	ND
Trans-2-hexenal	ND
2,4-Hexadienal	ND
Trans-2-octenal	ND
Trans-4-Phenyl-butene-2-one	ND
trans,trans-Hepta-2,4-dienal	ND
Ethacryanic acid	ND
p-nitrobenzyl chloride	ND
Cumene hyperoxide	ND
Hydrogen peroxide	ND

(ND: Not Detected)

4.7 Side directed Mutagenesis

Mutagenesis primers were constructed by introducing the nucleotides corresponding to alanine to replace the tyrosine codon at position 89 and 97. Mutagenic primers were designed using the web-based QuikChange Primer Design Program at www.agilent.com/genomics/qcpd (**Table 4.3**). Once the mutated clones were obtained, the purified mutant protein was subjected to specific activity assay, where the mutant protein showed much lower activity in comparison with the wildtype GSTD3 protein. As shown in **Table 4.4**, about 50 % of activity was lost in the mutated proteins. The significance on the protein reduced activity was further confirmed by looking at the Bradford protein quantification assay in **Table 4.5**, where the total protein content in all the three samples; wildtype GSTD3, mutant Y89A and Y97A, were equivalent.

Table 4.3: Mutagenic Primer-template duplexes

Primer Name	Primer-Template Duplex
Y89A	5'-tgatatggcgctgatggctccgaccctggcgaac-3' aaaactataccgcgactacataggctgggaccgcttgata
Y89A-antisense	ttttgatatggcgctgatgtatccgaccctggcgaactat 3'-actataccgcgactaccgaggctgggaccgcttg-5'
Y97A	5'-atccgaccctggcgaactattatgctaaagcgtttaccacc-3' acataggctgggaccgcttgataataatatttcgcaaatggtggccg
Y97A-antisense	tgtatccgaccctggcgaactattattataaagcgtttaccaccggc 3'-taggctgggaccgcttgataatacgatttcgcaaatggtgg-5'

Table 4.4: Specific Activity of wildtype and mutant GSTD3

Enzyme	Specific activity (µmol/min/mg)
Wildtype GSTD3	7.38 ± 0.42
Mutant GSTD3 Y89A	3.51 ± 0.09
Mutant GSTD3 Y97A	3.01 ± 0.15

The SDS gel image in **Figure 4.9** shows the crude expression of the mutant protein comparatively to the wildtype GSTD3. The induction with 0.3 mM of IPTG for 4 hours shows overexpression of GSTD3 protein in both wildtype and mutated clones at about 22 kDa.

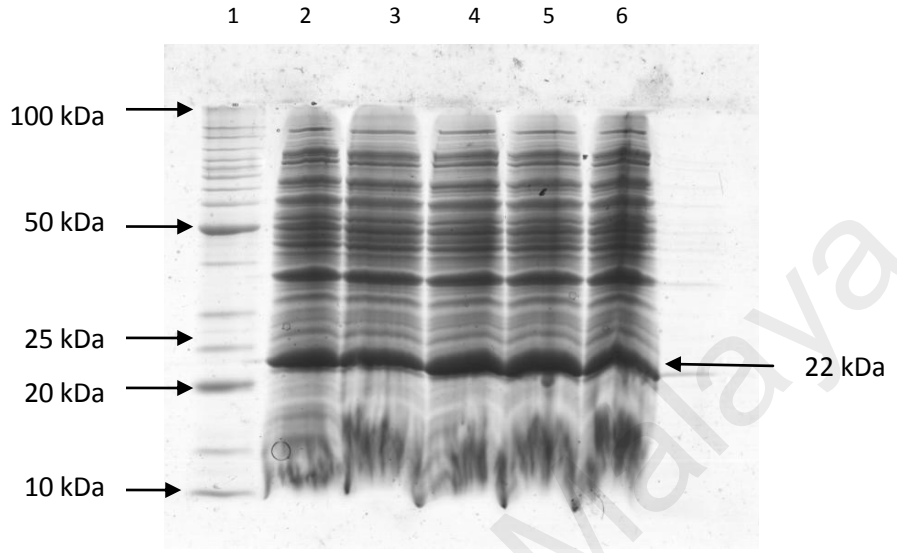

Figure 4.9 shows the SDS PAGE of crude protein extracted from the *E. coli* BL21 cloned with wildtype DmGSTD3 and also mutated DmGSTD3. The gel was stained using the colloidal coomasie blue staining method. Comparatively to negative control crude in **Figure 3.8** (Lane 2), the overexpression at about 22 kDa (indicated by an arrow) shows the expression of recombinant GSTD3 *in E. coli* BL21 DE3 pLysS.

Lane 1: 1 kb BenchMark Biorad
Lane 2: Crude lysate of *E. coli* BL21 cloned with DmGSTD3 wildtype
Lane 3: Crude lysate of *E. coli* BL21 cloned with DmGSTD3 mutant Y89A
Lane 4: Crude lysate of *E. coli* BL21 cloned with DmGSTD3 mutant Y97A
Lane 5: Crude lysate of *E. coli* BL21 cloned with DmGSTD3 mutant Y8997A
Lane 6: Crude lysate of *E. coli* BL21 cloned with DmGSTD3 mutant Y8997G

4.8 Circular Dichroism Spectroscopy

Circular dichroism technique is a useful to study the protein structure under the condition in which the protein actually operates, and providing the information on the structural change that the proteins adapt in order to function biologically. The circular dichroism spectra in the different regions can be used to know the structural relationship between the native and recombinant proteins also between wildtype and mutants enzymes (Kelly et al., 2005). Based on **Figure 4.10** the curve proved that there were no conformational changes in the mutant proteins when compared to the wildtype D3 protein.

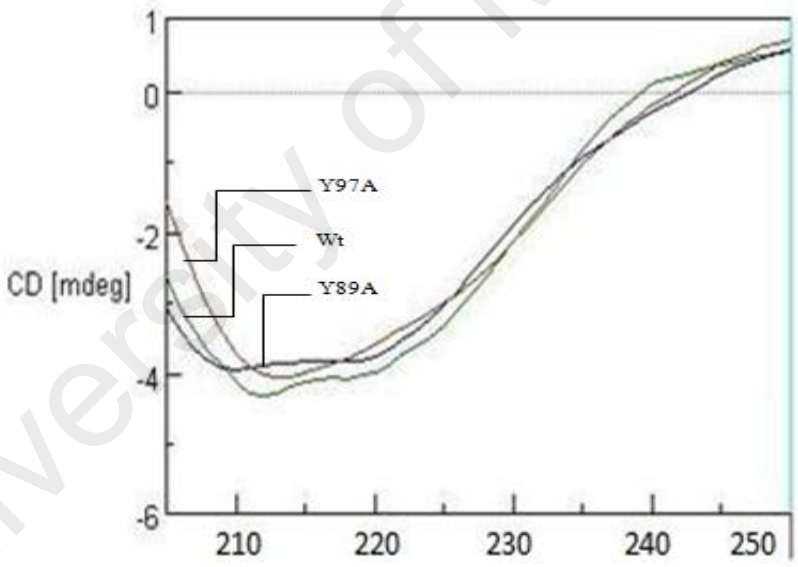

Figure 4.10 shows the CD spectroscopy chromatogram of the wildtype D3 protein compared with the mutant D3 proteins (Y97A and Y89A).

4.9 Inhibition Assay (IC_{50})

Inhibition assay was performed using few inhibitors namely; triphenyltin hydroxide, quercetin, *trans*-chalcone, tetradecanedioic acid, sebacid acid and triphenyltin acetate. Out of those, only triphenyltin hydroxide inhibited the activity of GSTD3 with CDNB (1 mM) and GSH (1 mM). The concentration of the triphenyltin hydroxide at where 50 % of the inhibiton was observed (IC_{50}) was 0.53 mM. According to the graph (**Figure 4.11**), IC_{50} of triphenyltin hydroxide was 0.53 mM (indicated with a dashed arrow).

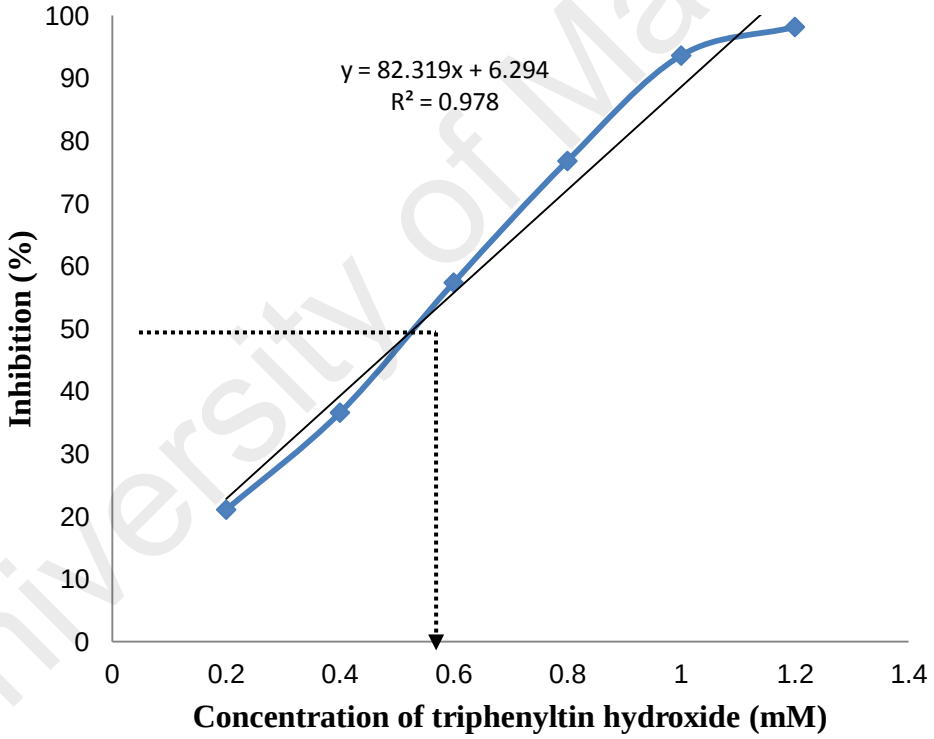

Figure 4.11 shows the inhibition of GST activity by different concentration of triphenyltin hydroxide. The dashed arrow indicates the IC_{50} of triphenyltin hydroxide at 0.53 mM

4.10 Effect of temperature on GSTD3 activity

Temperature effect on GSTD3 activity was investigated at the range of 15 to 42°C. Optimal temperature was at 25°C and almost no activity was detected at 42°C. Thermostability was determined by preincubation of the enzyme mixture at various temperatures for 15 min before activity was assayed at pH 6.5. The graph of GSTD3 enzyme rate plotted against different temperature. Base on the curve (**Figure 4.12**), the highest D3 protein activity was at 25°C with the rate of 154.136 s^{-1}.

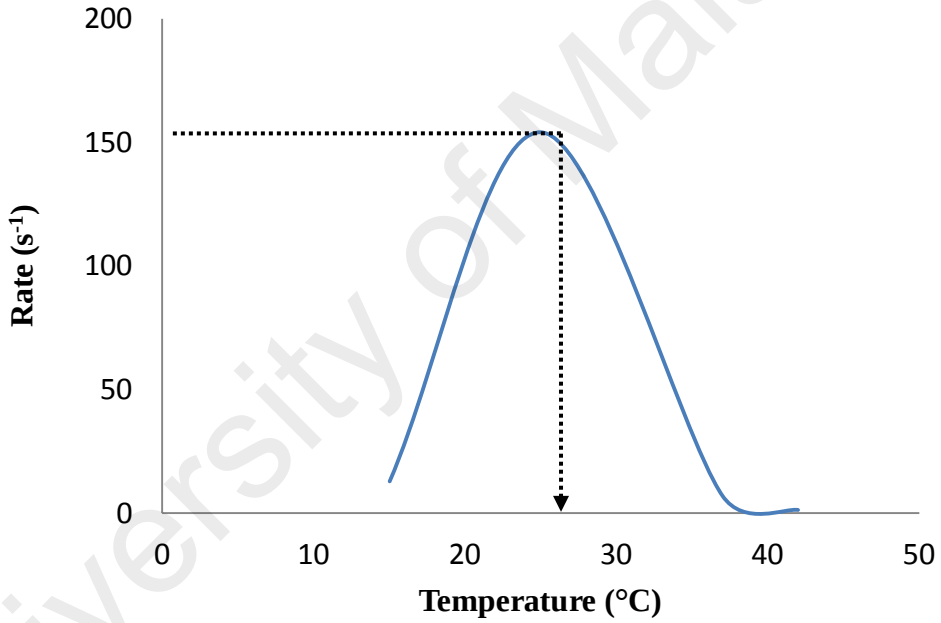

Figure 4.12 shows thermostability of DmGSTD3. As indicated by the dashed arrow, the highest activity was at the 25 °C.

4.11 Effect of pH on GSTD3 activity

The effect of pH on the GST activity was investigated by using different pH natured buffer like citrate-phosphate buffer (pH 3-pH 6), sodium phosphate buffer (pH 6-8) and tris hydrochloride buffer (pH 8-9). GSTD3 activity had an optimum pH at pH 8.2 but a sharp decrease at pH 9. This sharp decrease has been observed with other GSTs as well (Plancarte et al., 2004). The graph of GSTD3 enzyme rate plotted against different pH. Base on the curve (**Figure 4.13**), the highest D3 protein activity was at pH of 8.2 with the rate of 625.817 s^{-1}.

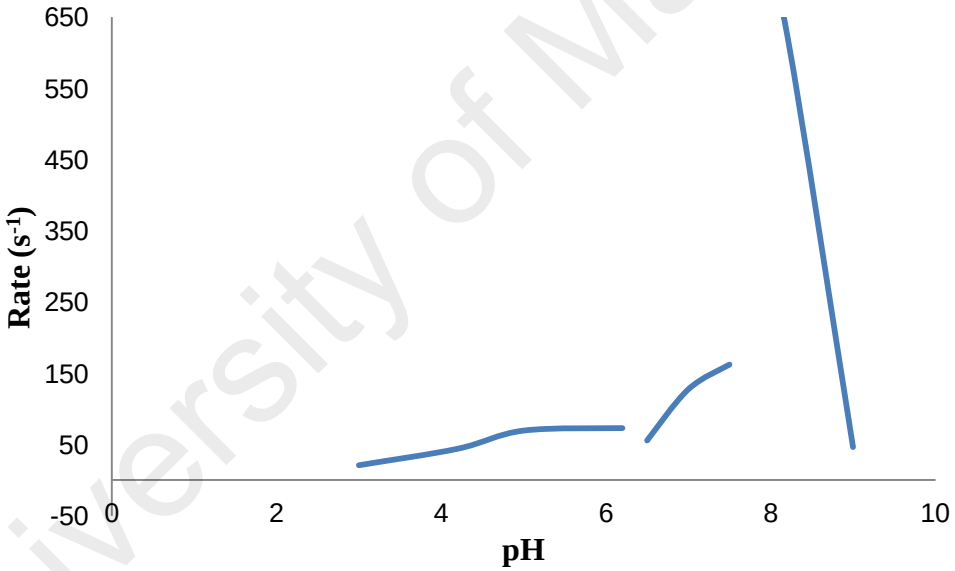

Figure 4.13 shows optimal pH of DmGSTD3 assayed using citrate–phosphate–tris buffer at various pH conditions at 25 °C. pH range of each buffer; citrate-phosphate buffer (pH 3-pH 6), sodium phosphate buffer (pH 6-8) and tris hydrochloride buffer (pH 8-9).

4.12 Kinetic Characterization

Observation on the different kinetic parameters of the GSTD3 wildtype and mutant protein towards CDNB is shown in **Table 4.6.** Maximum velocity was obtained using the Sigmaplot 12.2 software by providing the initial velocity of the GSTD3 wildtype and mutant proteins at varying concentration of GSH and CDNB. The kinetic measurement assay for CDNB and GSH was carried out independently; varying CDNB concentration (0.4 mM-1 mm), fixed GSH (1 mM) and varying GSH (0.4 mm-1 mm), fixed CDNB (1 mM).

The Michaelis-Menten equation was adopted to calculate the rate constants involved in the initial reaction rate under steady state conditions. K_m, K_{cat} was then deduced from maximum velocity (V_{max}) obtained from the Sigmaplot. K_m has an inverse relationship to substrate's strength in binding to an enzyme, hence is a measure of the substrate affinity towards the the binding site on the enzyme. The tighter the binding, the lower the K_m gets. Kinetic study of GSTD3 wildtype and mutant proteins show tremendous increase in K_m for both mutants, Y89A and Y97A (1.6 and 2 fold respectively) when GSH concentration was varied. This shows that Tyr97 plays a role in increasing the affinity of GSTD3 towards the active site of the CDNB.

The turnover number or the molecular activity is denoted by K_{cat}. The K_{cat} value was the lowest in the mutant Y97A, about 55 % lower than wildtype. This suggests that the absence of Tyr97 affects the catalytic efficiency of the GSTD3 in a higher lever compared to Tyr89. In order for a chemical reaction to occur in between two molecules, there has to be a collision involved. K_2 ($M^{-1}s^{-1}$) is a biomolecular rate constant representing this second order velocity proportionate to the concentration of

the two molecules. The K_2 value for the reaction of GSTD3 and its substrate was $0.000467 \pm 0.000001\ M^{-1}s^{-1}$.

The free energy (Gibbs energy, G) calculated shows that GSTD3 is involved in an endergonic reaction with CDNB and GSH, and the mutation of the Tyr89 and Tyr97 seemed to have caused a increase in free energy in the its process towards reacting with GSH.

Table 4.5: Kinetic parameters of wildtype (wt) and mutants (Y89A and Y97A) expressed in *E. coli* BL21 as determined using selected substrates (CDNB and GSH)

	V_{max} µmol/min/mg			K_m mol/L			K_{cat} s^{-1}			K_{cat}/K_m $(mol/L)^{-1}$ s^{-1}		
	wt	Y89A	Y97A	wt	Y89A	Y97A	wt	Y89A	Y97A	wt	Y89A	Y97A
CDNB	25.72±4.11	13.15±2.49	10.87±3.09	2.77±0.49	2.60±0.63	2.32±0.89	1.29±0.21	0.64±0.12	0.52±0.15	0.466	0.247	0.226
GSH	27.46±7.31	5.48±2.01	7.24±1.01	2.66±1.07	**4.28±2.10**	**5.57±1.01**	1.38±0.37	**0.27±0.09**	**0.35±0.05**	0.519	**0.0627**	**0.063**

	Free energy (kJ/mol)	
	Y89A	Y97A
CDNB	1.56	1.79
GSH	5.23	5.23

5.0 DISCUSSION

5.1 Cloning and expression of DmGSTD3 gene

Dmitri (2002) has reported that *D. melanogaster* goes through DNA loss and deletions at a highest rate, which also contributes to its very compact and 'junk-free' genome. These mutations that happen along with natural selection can cause gene evolution in many important ways. Natural selection has been said to direct evolution by sorting random variants based on their adaptive values. Basically, pseudogenes are the non functional copies of functional genes which evolved without the functional constraints in a spontaneous mutation pattern. The deletions found in Drosophilae is said to have a very high rate and long deletions when compared to mammals and other insects (Dmitri, 2002).

The N-terminal deletions has been the main reason why DmGSTD3 gene to be presumed as a pseudogene by Toung et al. (1993). But that conclusion was proven wrong by Sawicki et al. (2003), who showed that the gene was functional to atleast at the transcript level. In order to further characterize and study the DmGSTD3, the gene has to be cloned and expressed *in vitro*. The target gene sequence has to be amplified from the whole genome of *D. melanogaster* so that it can be expressed in an *E. coli* expression system, with a controlled environment. Polymerase chain reaction was carried out to amplify the *DmGSTD3* gene using specific primers that were commercially synthesized. The suitable annealing temperature was optimized to 55 °C as it produced single amplified band of *DmGSTD3* gene in large amount. After amplification, PCR product was analysed on 1% agarose gel. The band was about 700 bp (**Figure 4.2**). The band was either gel purified or purified using a PCR purification

kit. The PCR purification kit is a more favorable means of DNA purification as it gave high yield of purified DNA compared to gel purification. But, the usage of PCR purification kit is not encouraged if the purified DNA is to be sent out for sequencing. So, when gel slicing step is concerned, precaution steps has to be taken to make sure the DNA is exposed to UV for less than 20 seconds. The harmful UV exposure during the gel slicing step in gel purification could denature the nucleotides at the TA terminal thus disrupting the blunt end ligation process.

Two types of vector plasmids were used in order to construct a well expressed recombinant protein of GSTD3 in large quantity. First a high copy number vector was used, pGEMT Easy (**Figure 5.1**). This vector allows blunt end cloning with TA overhangs facilitating easier digestion using restriction enzyme for gene excisions. Blunt end cloning is a much more easy yet versatile method because it skips the enzymatic digestion and the subsequent purification prior to ligation which can affect the nucleotides during to the UV exposure. But the disadvantage of the cloning method is that it results in fewer colonies and also a lot of plasmid recirculation. In order to reduce the risk of picking the non recombinant clones, blue white screening method was used (Sambrook and Russell, 2001). The blue white screening method is applicable in a vector that has the ability to code for a β–galactosidase enzyme producing gene, *LacZ*. β–galactosidase functions in metabolizing galactose to lactase and glucose. So, when X-gal (5-bromo-4-chloro-3-indolyl-[beta]-D-galactopyranoside) was added in the growth medium, β–galactosidase metabolizes X-gal resulting in bright blue products. At the same time, the *LacZ* gene contains multiple cloning sites where the DNA fragments can be inserted into, in a way deactivating the gene from producing the enzyme. This phenomenon is called ‘insertion inactivation’. Hence, the clones’ colony appears white on the plates, thus facilitating in recombinant plasmid identification.

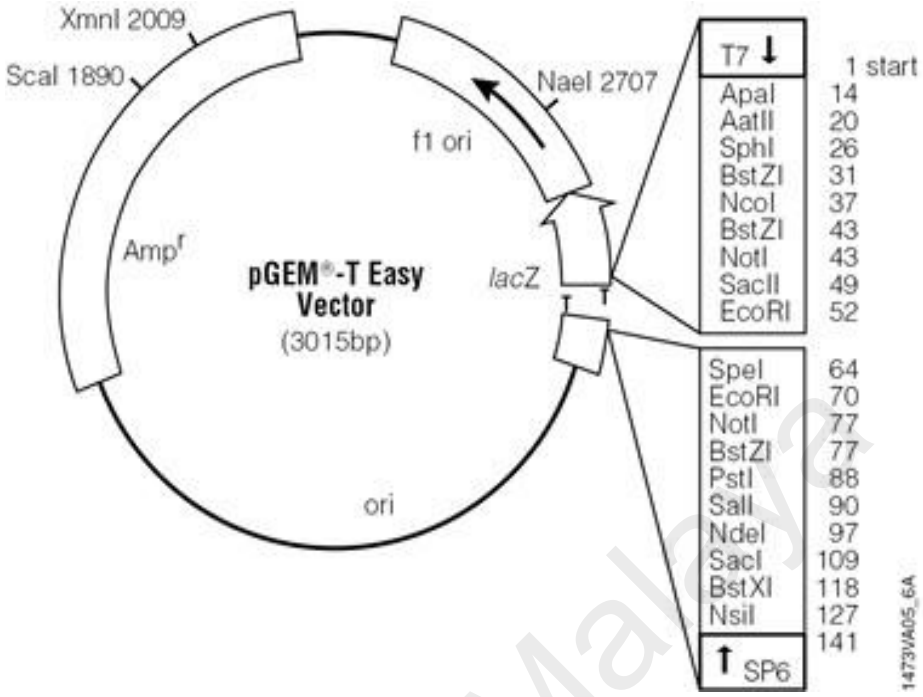

Figure 5.1 shows the pGEMT Easy Vector map with the multiple cloning site and restriction sites for easy digestion and excision of gene of interest.

Once pGEMT-D3 clones were obtained, the genes were sequenced using the T7 promoter universal primers. To confirm the identity of the cloned gene the sequenced nucleotide was matched with the database in NCBI (BLAST). As shown in **Figure 4.5**, the sequenced result which is the query sequence had 100% similarity with the *Drosophila melanogaster* gluthatione S transferase D3 (NM 176479.2).

With the sequencing results being positive, the gene of interest was then excised from the pGEMT Easy vector and was ligated into an expression vector, pET30a(+) (**Figure 5.2**). Restriction enzymes were chosen by comparing the non-cutters and cutters of the gene sequence of *DmGSTD3* gene and pET30a(+) vector; *Nde*1 and *EcoR*1 sites were chosen in our case. The pET30a(+) was chosen as the expression vector as many studies proved to have successfully cloned GSTs with well expressed protein production. For example, the cloning of a pi-class GST from freshwater mussels *Cristaria plicata* (Hu et al., 2012) and GSTs from *D. melanogaster* (Sawicki et al., 2003). No tags, like His-tag, were added to the *E. coli* expression system that could actually aid purification to avoid side effects of the tags at the N terminal region (Yamamoto et al., 2011). The pET30a(+) is one of the best vectors known for its good expression level because it uses the T7 promoter system that can be induced by adding IPTG. The reason using the pET30a(+) for the cloning was due to its advantage of having T7 promoter for over expression. Besides it having the restriction enzyme sites would make it possible for the work to avoid relegation of the vector during the ligation.

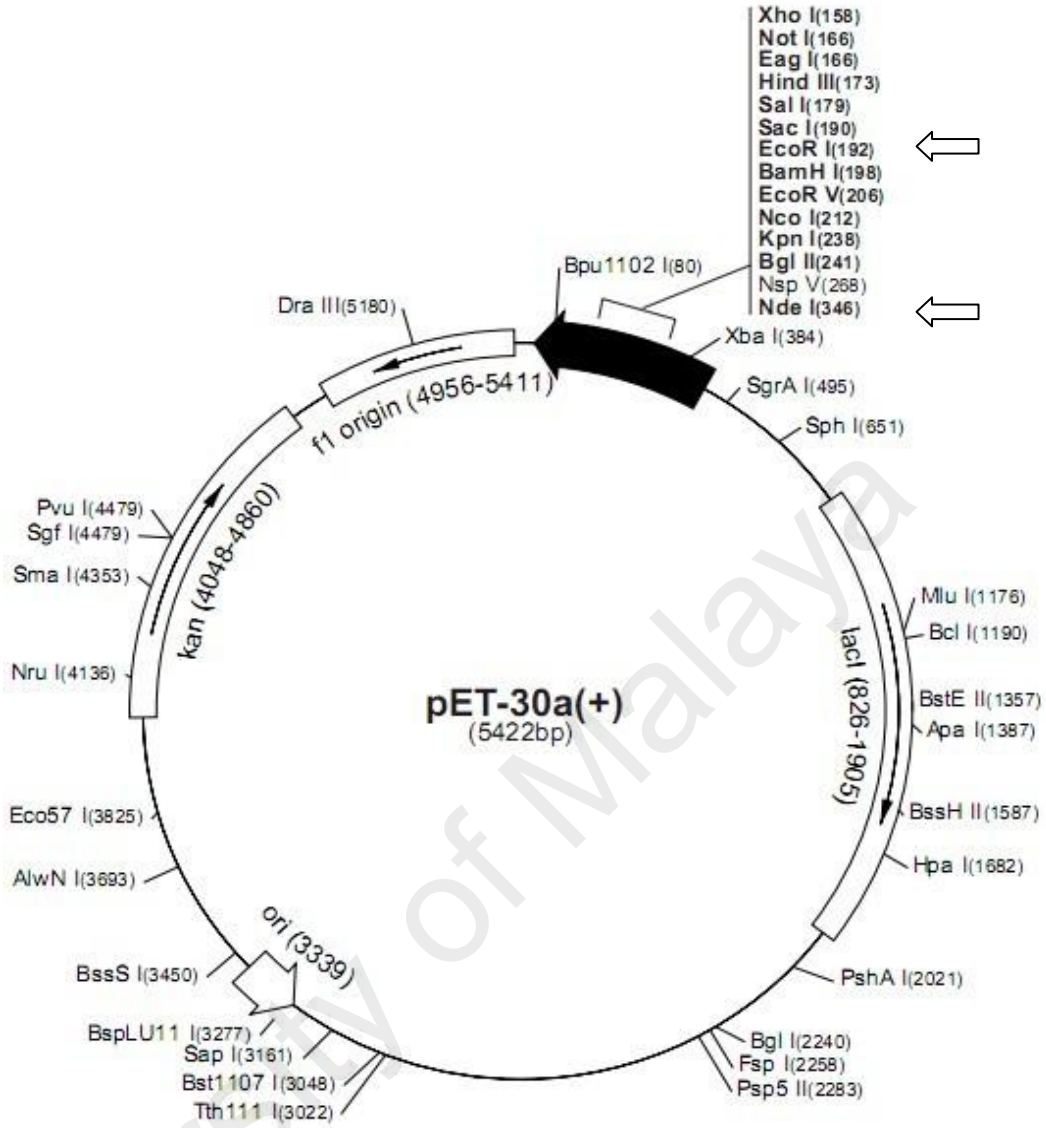

Figure 5.2 shows pET-30a(+) Vector map showing the multiple cloning site with restriction sites. The restriction sites that were chosen to insert the gene of interest are indicated with an arrow.

Next, the vector was ligated with the insert using the Clonable 2X Ligation Premix kit as per the manufacturer's instruction. The clones were transformed into *E. coli* host. The competent cell used provides a range of expression when used with T7 promoter driven vectors. This expression system was reported to be used in the cloning and expression of delta class GSTs in *D. melanogaster* earlier by Sawicki et al., (2003) and epsilon class GSTs in *Anopheles Cracens* by Wongtrakul et al., (2009).

Transformed *E. coli* was spread on LB agar plate containing kanamycin (30mg/ml) and incubated at 37 °C overnight. Cells that contained pET30-GSTD3 were able to grow in the LB with kanamycin media due to the presence of the kanamycin resistant gene (Kan^R) in the vector. Thus, this was the method of selection of the cloned cells used before further protein analysis.

Ten random colonies were picked and cultured in LB broth containing kanamycin. Plasmids were extracted from the bacterial pellet using plasmid extraction kit. The extracted plasmid was loaded into 1 % (w/v) agarose gel to check for purity and size. Four bands were visualized on the gel at approximately 6000 bp and higher (**Figure 4.4**). These multiple bands of plasmids represent the different form of plasmids; nicked, coiled, linearized and supercoiled structure of plasmids that move in different time rates during the gel electrophoresis. Once the size has been confirmed, the purified plasmid was then double digested and the mixture was loaded into 1 % (w/v) agarose gel to check if the plasmid contains the target gene, i.e insert. Besides the digestion method of verification, the extracted plasmid was used as a template to perform PCR using the DmGSTD3 specific primers. The PCR product was then loaded on 1 % (w/v) agarose gel once again to check if there was any gene amplified and a single band at 700 bp (**Figure 4.4b)** was observed.

Once the recombinant plasmid and transformant *E. coli* colony with the recombinant gene has been identified, the particular colony was cultured in 500 ml of LB medium. This large scale culturing was to allow the GSTD3 protein expression. The protein expression was induced by the addition IPTG at the concentration of 0.3 mM which was added to the overnight culture for not more than 4 hours of induction at 37 °C. After that, the cells were harvested via centrifugation and the cells were lysed to obtain the expressed proteins since it is an intracellular expression. This was confirmed by running activity assay with the cultured medium (extracellular), cell lysis debris (membrane-bound) and lysate (intracellular). Activity with CDNB was only detected with the lysate of the *E. coli*-GSTD3 cells.

5.2 Purification of GSTD3

GSTD3 was purified using the ion exchange, Q-HP. Since the pI value of GSTD3 is 4.8, hence buffer with pH above 6 was suggested to be used in order to trap the protein using the anion exchange. At pH above pI value the protein would bind to a positively charged medium or anion exchanger. The anion exchanger chromatography is a technique where charged molecules bind to the separation medium at low ionic strength and then eluted with salt. It separates molecules on the basis of the difference in their net surface charge. The charged groups within a molecule that contribute to the net surface charge possess different pKa values depending on their structure and chemical environments. It's highly pH dependant.

After a few purification optimizations, pH 8 was selected for the phosphate buffers used in the experiment for eluting out the proteins. The pH and ionic strength of the buffer were selected to ensure that most of the protein of interest binds to the matrix leaving behind the impurities to be washed out from the system to the waste flask. The purified protein was then reconfirmed through enzyme assays using glutathione and other substrates and SDS PAGE to determine the size of the purified protein.

Before loading the lysate into the AKTA system, activity towards CDNB was assayed to make sure the crude lysate has the expressed protein extracted well from the *E. coli* cells. In order to confirm the fraction that contains the most protein eluted, activity assay was run with each fraction separately. Then the fractions with activity towards CDNB were loaded on a SDS PAGE (14 %) gel to check for the most purified fraction. The fractions with almost clear single band were all pooled together and freeze-dried for future use.

As shown on **Figure 4.8**, the crude lysate shows a thick protein band at the molecular weight of 22 kDa, which matches the GSTD3 deduced size. Once purified, 0.5 M NaCl elution gave a single band of 22 kDa as well. This condition was fixed for the other mutant enzymes purification. The analysis of SDS-PAGE photo and R_f vs LogMW graph showed that the GSTD3 enzyme consisted of single subunits of M_r 22.4 kDa.

5.3 Catalytic Activity and Role of GSTD3

Substrate specificity showed that the purified GSTD3 showed activity only with CDNB (7.38 μmol/min/mg). This is a common substrate for the delta class GSTs. Nevertheless, Sawicki et al., (2003) reported that GSTD3 showed activity with HNE, which means GSTD3, is involved in lipid peroxidation. But, when assayed with other lipid peroxidization by products like 2,4-hexadienal and *trans*-2-octenal, no activity was detected. This shows that the enzyme is specific to only certain type of lipid peroxidation products only.

It has been previously reported that GSTD3 transcriptome are mostly detected during the larvae or pre adult stage. The conjugation with 4-HNE proves the function of GSTD3 in a variety of physiological conditions like embryogenesis and metamorphosis. This is because 4-HNE has signalling functions affecting cell proliferation, differentiation and apoptosis, thus GSTD3 probably modulate and terminate these functions of 4-HNE (Sawicki et al., 2003).

Meanwhile, Wongtrakul et al., (2012) suggested a role for DmGSTD3 in p38 MAPK signalling because DmGSTD3 interacted with p38b and increased Jun

phosphorylation rates 2.6 fold, indicating a non catalytic role of DmGSTD3 in the modulation of p38b. This hypothesis was further justified when it has been reported that over expression of GSTD3 was observed when treated with paraquat by Alias and Clark (2007). Paraquat is a potent herbicide that produces reactive oxygen species (ROS) during a cyclic reaction with oxygen. ROS damages cell and results in lipid peroxidation products (Wongtrakul et al., 2012). Work by Alias and Clark (2007) has demonstrated the expression of GSTD3 was induced by the paraquat treatment. This observation suggests that GSTD3 could have played role in oxidation stress response. A further supporting incident was also demonstrated by Sawicki et al. (2003). Recombinant GSTD3 has activity towards 4-HNE, a lipid peroxidation product (Sawicki et al., 2003).

To determine the catalytic properties, turn over number (K_{cat}), and catalytic efficiency (K_{cat}/K_m) with respect to glutathione and CDNB were calculated. This study of enzyme catalytic reaction measures the rate of reaction and the mathematical constants (Rogers and Gibon, 2009). V_{max} and K_m values were determined by the Michaelis-Menten equation. Besides that, further characterization was performed in order to know the catalytic behaviour of the enzyme like the optimal pH and temperature for the enzyme stability during catalysis. The bonds that hold proteins in their secondary and tertiary structures are disrupted by changes in temperature and pH. While, extreme pH can result in denaturation of folded structure due to repulsive forces, milder pH can dissociate the enzyme from its oligomeric state into inactive monomers.

The highest activity was observed with Tris-HCL buffer at pH 8.2. The activation energy has been reported previously for invertebrate GSTs (Ragaa et al.,

2005). At pH higher than 8.2, the activity of the enzyme dropped drastically, indicating that extreme alkalinity tempers the catalytic nature of the enzyme. This was either due to the pH affecting the shape of the enzyme or changes the shape and charge properties of the substrate. The optimal temperature was 25 °C, which was the temperature used during all enzyme assays for kinetic studies. This is usually the optimal temperature for invertebrate and plant enzymes.

5.4 Inhibition studies

Six inhibitors of different nature were screened for their inhibitors effect on GSTD3. The inhibitors include triphenyltin hydroxide, quercetin, *trans*-chalcone, tetradecanedioic acid, sebacid acid and triphenyltin acetate. Quercetin also known as pentahydroxyflavone, is a phytochemical, flavonoid. Chalcones are precursors of open chain flavonoids and isoflavonoids present in edible plants, a biosynthetic product of the shikimate pathway (Rahman, 2011). The others are known fungicide or herbicides commonly used.

Out of all six inhibitors, only triphenyltin hydroxide inhibited the GSTD3 catalysis. Hence, the IC_{50} which is the concentration of triphenyltin hydroxide that is needed to achieve atleast 50% inhibition on the GSTD3 was deduced from the **Figure 4.11** curve. In other words, IC_{50} is a quantitative measurement indicating the effectiveness of a substrate inhibiting an enzymatic reaction at a fixed concentration of substrate, which is the half maximal inhibitory concentration (Copeland, 2000).

5.5 Side directed mutagenesis

The catalysis of GST enzyme consists of several steps; glutathione ionization by thiol deprotonation, nucleophilic attack of the thiolate for substrate conjugate, product formation and release of the formed product from the active site (Vararattanavech and Ketterman , 2007). There are numerous reports on non active site residues that also play a role in the catalytic properties of enzymes through folding and stability. For example, in the alpha class, Phe51 is seen to stabilize the dimeric protein conformation through the lock and key interaction (Wongtrakul et al., 2003)

Apart from that, it is also understood that delta class adopts a different glutathione activation mechanism compared to other GST classes. The thiol proton is captured by an internal base residue at high pH in delta GSTs, unlike mu, alpha and pi GSTS where the thiol proton is released into the solution after the forming of thiolate anion. Ser9 has been reported to be involved in the stabilization of the ionized glutathione (Winayanuwattikun and Ketterman, 2004). But clearly, for the case of GSTD3, Ser9 is missing.

BLAST results correspond to GSTD3 from *D. melanogaster* with the length of 199 amino acids. From the reference sequence, the GST N-terminal region can be found at position 1 to 58 and the C-terminal at position 72 to 88. Glutathione binding position is predicted to be at 34 till 49 position coding His, Ser, Ile, Glu and others. Substrate binding pocket is located at 85 to 187. G site is usually common for all GST classes, whereas the H site is different between classes and isoforms. **Figure 4.7** shows the structure of ligand (glutathione) binding into the N-terminal domain of GST isoform 1. From model visualization, there were few tyrosine residues adjacent to the

GSH binding site at 82, 89, 95, 96 and 97 positions. Side chains of 89 and 97 were projecting inside into the glutathione binding site. Referring to the force field calculated it shows that Tyr97 is a more suitable residue with lower energy. Vararattanavech and Ketterman (2007) identified a Tyr residue at the position 5 or 6 to be responsible with deprotonation and stabilization of ionized glutathione in alpha, mu and pi GST classes. Hence, these two residues were hypothesized to be compensating the missing conserved Ser or Tyr residue.

This tyrosine residue near the active site of glutathione is predicted to be involved in the 'base assisted deprotonation model' for glutathione ionization. Vararattanavech and Ketterman (2007) have explained that the 'base assisted deprotonation' is a mechanism of GST enzyme where glutathione reacts as a catalytic base in the thiol proton acceptance from the glutathione thiol group. The electron distribution stabilizes the ionized thiol of glutathione, hence showing the involvement of glycine in glutathione ionization. The glycine moiety involvement was observed in AdGSTD4-4, where His38 mutagenesis resulted in the decrease in binding affinity of glutathione as well as the enzyme catalytic rates (Vararatanavech and Ketterman, 2007).

To investigate the roles of the Tyr residues in the catalysis of GSTD3, mutagenesis studies were carried out in order to characterize the engineered GST through kinetic constants and substrate specific activity. The Tyr at 89 and 97 were mutated to alanine because its side chain consist of hydrogen would make the enzyme not to able to carry out the catalytic activity without a catalytic residue. All the mutated genes were expressed in soluble form similar to the wildtype GSTD3 gene. Both Y89A and Y97A purified protein showed low activity towards CDNB (3.51 μmol/min/mg and

3.01 μmol/min/mg respectively). Besides these two mutants, another two mutants were constructed by mutating both 89 and 97 tyrosine to either alanine (Y89/97A) or glycine (Y89/97G). But no further studies were conducted due to the failure to obtain pure proteins. This also might suggest the loss of altered characteristic of the mutant protein compared to the wildtype. The crude expression of these two mutants was shown in **Figure 4.9**.

Several studies has been demonstrated that a single change in amino acid outside the active site can affect the catalysis of GSTs due to their role in folding and stability of the dimeric conformation through lock and key intersubunit interaction (Wongtrakul et al., 2003). Certain residues play a minor role in structural integrity where the replaced residues would induce changes in the active site topography hence reducing the activity (Vararatanavech and Ketterman, 2007). To make sure that the lowered activity is solely due to the absence of the Tyr and not due to any conformational or structural differences, circular dichroism spectroscopy test was carried out.

Circular dichroism was performed to determine whether secondary structure content of the proteins had changed. It gives a picture of two 'troughs' at 210 and 222nm, showing the high helical content of the proteins (Vararatanavech et al., 2006). It's a valuable technique for examining the structure of protein in solutions, which is the condition the particular protein, actually operates thus providing the measures of the rates of structural changes of proteins, essential to their biological functions. Circular dichroism refers to the different absorption of two circularly polarized components of equal magnitude, one rotating counter- clockwise (L) and another clockwise (R) (Kelly et al., 2005).

All three; wildtype, Y89A and Y97A, gave a similar curve pattern proving the mutants and wildtype D3 have the same conformations (**Figure 4.10**). This proves although some mutations affect the catalysis, the overall secondary structure content of the enzymes has not been altered. From the CD spectrum, even though the mutants were similarly structured with the wildtype, it seemed that the mutant protein Y97A was more properly folded and rigid when compared with the wildtype. Whereas, Y89A had slight changes where α-helix content seemed to be lesser compared to the wildtype. Besides that, Kelly et al. (2005) suggested that dialysis or gel permeation should be carried out prior to measurement to remove protective agents or buffer ions used to elute proteins from the ion exchange columns. This is because the impurities would give high absorbance in the UV region hence an irregular pattern.

Circular dichroism data also is invaluable for the knowledge on the expressed domain integrity in multidomain protein. Besides that, the loss of if CD signals due to the denaturants like urea or guanidium or high temperature provides quantitative estimates of native protein folded state stability. In order to subject a protein to circular dichroism technique, the sample has to be produced by over expression of the gene encoding for the particular protein with a suitable host system, and the protein should be purified for atleast 95% purity as seen on SDS PAGE

5.6 Kinetics studies

This study of enzyme catalytic measures the rate of reaction and the mathematical constants (Rogers and Gibon, 2009). The V_{max} and K_m values were determined by the Michaelis-Menten equation. According to the **Table 4.6**, Y89A and Y97A enzymes gave large changes in V_{max} and K_m towards both substrates; CDNB and GSH.

V_{max} was affected in a higher level with GSH, about 4-5 folds, whereas about 2 fold towards CDNB. K_m values towards CDNB were not affected much between the wildtype and mutants. But vast difference in the K_m value of GSH in the mutants compared to wildtype D3; 1.6 fold in Y89A and 2.2 fold in Y97A. K_m values show the affinity of the enzyme towards a substrate.

This somewhat proves that Tyr89 and 97 residues play a role in GSH substrate binding with the GSTD3. Y97A seemed to have lower affinity towards GSH compared to Y89A. Thus it can be said residue Tyr97 is much more important in GSH stabilization. This might be because Tyr97 position is more stable base on the force field energy compared to Tyr89.

The increase in K_m value means that higher substrate concentration is needed to achieve the given velocity. The comparison of the V_{max} and K_m values show that Tyr97 is more important in the stabilization of glutathione. Besides that, the K_{cat}/K_m values of both mutants were low compared to the wildtype. K_{cat}/K_m reflects the catalytic efficiency of the enzyme, where how fast the enzyme reacts with substrate is shown with specificity constants. Based on table 4.6, the K_{cat}/K_m value was affected badly

towards GSH in both the mutant enzymes, 8.5 fold lower in comparison with the wildtype enzyme. And only 1.8 fold lower compared to wildtype towards CDNB. Thus it can be said that the Tyr residues is a 'base assisted deprotonation model' for glutathione ionization. In the wildtype enzyme, the conjugation of glutathione increases the solubility of the target molecule thus facilitating the excretion of the molecule (Vararatanavech and Ketterman, 2007).

6.0 CONCLUSION

Based on our studies, it can be clearly said that the glutathione S transferase delta class 3 from the *D. melanogaster* is definitely not a pseudogene. The GSTD3 gene was expressed and proved to be a delta class GST enzyme base on the activity exerted towards glutathione and CDNB even with the truncated conserved amino acids. The recombinant DmGSTD3 has shown no activities towards 3,4-dichloronitrobenzene, 2,4-hexadienal, 2,4-heptadienal, 4-nitrobenzyl chloride, ethacrynic acid, transoctenal and hydrogen peroxide. This suggests its limited function and role in toxins detoxification in fruitflies. The characterization studies on the GSTD3 enzyme showed that it's most optimal temperature was at 25 °C and pH 8.2. Based on the structural studies and directed mutagenesis, the missing conserved amino acid seemed to be replaced by the two potential tyrosine at the position 89 or 97. Kinetic pattern reflects that the Tyr97 and Tyr89 play an important role in the GSH conjugation to substrate. Besides that, the major reduction in specific activity values also defines the significant role of the two tyrosine positions in the GSTD3 enzyme. To confirm the structural position of the Tyr89 and Tyr97, x-ray crystallography should be modulated. Further investigation is recommended to evaluate the biological function of GSTD3 other than of normal detoxification function. In depth study of the GSTD3 from the *D. melanogaster* will be very applicable in the development of biosensors and in insecticide-resistance management strategies for agricultural pests.

7.0 REFERENCES

Alias, Z. and Clark, A.G. (2007). Studies on The Gluthathione S-transferase Proteome of Adult *Drosophila melanogaster*: Responsiveness to Chemical Challenge. Proteomics, 7: 3618-3628

Armstrong, R.N. (1997). Structure, Catalytic Mechanism and Evolution of the Glutathione Transferases. Chemical Research in Toxicology, 10(1): 2-18

Ayres, C.F., Muller, P., Dyer, N., Wilding, C.S. and Rigden, D.J. (2012). Correction: Comparative Genomics of the Anopheline Glutathione S-Transferase Epsilon Cluster. PLoS ONE 7(1): 10.1371

Ben-Arie, N., Khen, M. and Lancet, D. (1993). Glutathione S-transferases in Rat Olfactory Epithelium: Purification, Molecular Properties and Odorant Biotransformation. Biochemical Journal, 292: 379-384

Bradford, M.M. (1976). A Rapid and Sensitive for the Quantitation of Microgram Quantitites of Protein Utilizing The Principle Of Protein-Dye Binding. Analytical Biochemistry, 72: 248-254

Brophy, D.M., Southan, C. and Barrett, J. (1989). Glutathione Transferase in the Tapeworm *Moniezia expansa*. Biochemical Journal, 262(3): 939-946

Copeland, R.A. (2000). Enzymes: A Practical Introduction to Structure, Mechanism and Data Analysis. New York: Wiley-Verlag Chemie

Dixon, D.P., Skipsey, M. and Edwards, M. (2010). Roles for Glutathione Transferases in Plant Secondary Metabolism. Phytochemistry, 71: 338–350

Dmitri A.P. (2002). DNA Loss and Evolution of Genome Size in *Drosophila*. Genetica, 115: 81–91

Enayati, A.A., Ranson, H. and Hemingway, J. (2005). Insect Glutathione Transferases and Insecticide Resistance. Insect Molecular Biology, 14(1): 3-8

Gaelle, L.G., Freferique, H., Blair, D.S., Sam, B. and Eric, W. (2006). Xenobiotic Response in *Drosophila Melanogaster*: Sex Dependence of P450 and GST Gene Induction. Insect Biochemistry and Molecular Biology, 36: 674–682

Guengerich, F.P. (1990). Enzymatic Oxidation of Xenobiotic Chemicals. Chemical Rubber Companies Critical Review Biochemistry Molecular Biology, 25: 97-153

Guengerich, F.P. (1991). Oxidation of Toxic and Carcinogenic Chemicals by Human Cytochrome P-450 Enzymes. Chemical Research Toxicology, 4: 391–407

Habig, H., Pabst, M.J. and Jacoby, W.B. (1974). Gluthatione *S*-Transferases: The First Step in Mercapturic Acid Formation. Journal of Biological Chemistry, 249: 7130-7139

Hu, B., Deng, L., Wen, C., Yang, X., Pei, P., Xie, Y. and Luo, S. (2012). Cloning, Identification and Functional Characterization of Pi-Class Glutathione S Transferase from the Freshwater Mussels Cristaria Plicata. Fish & Shellfish Immunology, 32: 51-60

Johansson, A.S. and Mannervik, B. (2001). Human Glutathione Transferase A3-3, a Highly Efficient Catalyst of Double-Bond Isomerization in the Biosynthetic Pathway of Steroid Hormones. The Journal of Biological Chemistry, 276: 33061–33065

Kelly, S.M., Jess T.J. and Price, N.C. (2005). How to Study Proteins by Circular Dichroism. Biochimica et Biophysica Acta 1751: 119 – 139

Ketterman A.J., Saisawang C. and Wongsantichon J. (2011). Insect Glutathione Transferases. Drug Metabolism Review, 43(2):253-65

Li, X., Zhang, X., Zhang, J., Zhang, X., Starkey, S.R. and Zhu, K.Y. (2009). Identification and Characterization of Eleven Glutathione S Transferase Genes from the Aquatic Midge *Chironomus Tentans* (Diptera: Chironomidae). Insect Biochemistry and Molecular Biology, 39: 745-754

Malena, A.N, and Bengt, M., (2011). Engineering GST M2-2 for High Activity with Indene 1,2 -Oxide and Indication of an H-Site Residue Sustaining Catalytic Promiscuity, Journal of Molecular Biology, 412: 111–120

Mannervik B. and Danielson U.H. (1988). Glutathione Transferases-Structure and Catalytic Activity. Chemical Rubber Companies Critical Review Biochemistry, 23(3):283-337

Motoyama, N., and Dauterman, W.C., (1980). Glutathione S-Transferases: Their Role in the Metabolism of Organophosphorus Insecticides. Reviews in Biochemical Toxicology 2, 49-69

Nair, P.M.G. and Choi, J. (2011). Identification, Characterization and Expression Profiles of *Chironomus Riparius* Glutathione S-Transferase (Gst) Genes in Response to Cadmium and Silver Nanoparticles Exposure. Aquatic Toxicology, 101: 550–560

Oakley, A. (2011). Gluthathione Transferases: A Structural Perspective. Drug Metabolism Reviews, 43(2): 138-151

Pal, R., Blakemore, M., Ding, M. & Clark, A.G. (2012). A Study of the Glutathione Transferase Proteome of *Drosophila Melanogaster*: Use of S- Substituted Glutathiones as Affinity Ligands, Affinity Chromatography. Sameh Magdeldin (Ed.), ISBN: 978-953-51-0325-7

Perry, T., Batterham, P. and Daborn, P.J. (2011). The Biology of Insecticidal Activity and Resistance. Insect Biochemistry and Molecular Biology, 41: 411-422

Plancarte, A., Rendon, J.L. and Landa, A. 2004. Purification, Characterization and Kinetic Properties of the Taenia Solium Glutathione S- Transferase Isoform 26.5Kda. Parasitology Research, 93: 137–144

Ragaa R.H., Mohamed R.A., Fawkia M.E, Abdel A.A. and Ola M.A. (2005). Purification and Characterization of a Glutathione S Transferase from *Mucor Mucedo*. Polish Journal of Microbiology, 54 (2): 153-160

Rahman, M.A. (2011). Chalcone: A Valuable Insight into the Recent Advances and Potential Pharmacological Activities. Chemical Sciences Journal, 2011: CSJ-29

Ranson, H., Rossiter, L., Ortelli, F., Jensen, B., Wang, X., Roth, C.W., Collins, F.H. and Hemingway, J., (2001). Identification of a Novel Class of Insect Glutathione S Transferase Involved in Resistance to DDT in the Malaria Vector *Anopheles Gambiae*. Biochemical Journal, 359: 295-304

Rogers, A., and Gibon, Y. (2009). Enzyme Kinetics: Theory and Practice In J. Schwender (Ed.), Plant metabolic networks, 71-104

Saisawang, C., Wongsantichon, J. and Ketterman, A.J. (2012). A Preliminary Characterization of the Cytosolic Glutathione Transferase Proteome from *Drosophila melanogaster*. Biochemical Journal, 442: 181–190

Sambrook, J. and Russell, D.W. (2001). Molecular Cloning: A Laboratory Manual. Cold Spring Harbor (3rd Edition), New York: Cold Spring Harbor Laboratory

Sandford, A.J. and Silverman, E.K. (2002). Chronic Obstructive Pulmonary Disease C 1: Susceptibility Factors For COPD The Genotype–Environment Interaction. Thorax, 57: 736–741

Sawicki, R., Singh, S.P.,Mondal, A.K., Benes, H., and B.J., Zimniak, P., (2003). Cloning, Expression and Biochemical Characterization of One Epsilon-class (GST-3) and Ten Delta-class (GST-1) Glutathione S- Transferases From *Drosophila melanogaster*, and Identification of Additional Nine Members of The Epsilon Class. Biochemical Journal, 370: 661-669

Sheehan, D., Meade, G., Foley, V.M. and Dowd, C.A. (2001). Structure, Function and Evolution of Glutathione Transferases: Implications for Classification of Non-Mammalian Members of an ancient Enzyme Superfamily. Biochemical Journal, 360: 1-16

Singh, M., Silva E., Schulze, S., Sinclair, D.A.R., Fitzpatrick, K.A. and Honda, B.M. (2007). Cloning and Characterization of a New Theta-Class Glutathione-*S*-Transferase (GST) Gene, *Gst-3*, from *Drosophila melanogaster*. Gene, 247: 167-173

Toung, Y.P.S., Hsieh, T.S., and Tu, C.P.D., (1993). The Gluthathione S- Transferase D Genes. A Divergently Organized, Intronless Gene Family in *Drosophila melanogaster*. Journal of Biological Chemistry, 268: 9737-9746

Townsend, B. (2003). Role of Glutathione-S-Transferase in Anti-Cancer Drug Resistance. Oncogene, 22: 7369–7375

Travensolo, R.F., Garcia, W., Muniz, J.R.C., Caruso, C.S., Lemos, E.G.M, Carrilho, E. and Araoujo, A.P.U. (2008). Cloning, Expression, Purification and Characterization of Recombinant Gluthathione-S-Transferase from *Xylella fastidioasa*. Protein Expression and Purification, 59: 153-160

Udomsinprasert, R., Bogoyevitch, M. and Ketterman J.A. (2004). Reciprocal Regulation of Glutathione S Transferase Spliceforms And The Drosophila C-Jun N-Terminal Kinase Pathway Components. Biochemical Journal, 383: 483-490

Vararattanavech, A. and Ketterman, A.J. (2007). A Functionally Conserved Basic Residue in Glutathione Transferases Interacts with the Glycine Moiety of Glutathione and is Pivotal for Enzyme Catalysis. Biochemical Journal, 406: 247–256

Vararattanavech, A., Prommeenate, P., and Ketterman, A.J. (2006). The Structural Roles of a Conserved Small Hydrophobic Core in the Active Site and an Ionic Bridge in Domain I of Delta Class Glutathione S-Transferase. Biochemical Journal, 393 (Pt. 1): 89-95

Vontas, J.G, Small, G.J., Nikou, D.C., Ranson, H. and Hemingway, J. (2002). Purification, Molecular Cloning and Heterologous Expression of A Glutathione S-Transferase Involved In Insecticide Resistance From The Rice Brown Planthopper, *Nilaparvata lugens*, Biochemical Journal, 362: 329-337

Vuilleumier, S. (1997). Bacterial Glutathione *S*-Transferases: What Are They Good for? Journal of Bacteriology, 1431–1441

Wan, Q., Whang, I., and Lee, J. (2008). Molecular Characterization of Mu Class Glutathione-S-Transferase from Disk Abalone (*Haliotis discus*), A Potential Biomarker Of Endocrine-Disrupting Chemicals. Comparative Biochemistry and Physiology, Part B, 150: 187–199

Wendel, A. (1981). Glutathione peroxidase. Methods in Enzymology, 77: 325–333

Winayanuwattikun, P. and Ketterman, J.A. (2004). Catalytic and Structural Contributions for Glutathione-Binding Residues in a Delta Class Glutathione S-Transferase. Biochemical Journal, 382: 751–757

Winayanuwattikun, P. and Ketterman, J.A. (2005). An Electron-Sharing Network Involved in the Catalytic Mechanism is Functionally Conserved in Different Glutathione Transferase Classes. The Journal of Biological Chemistry, 31776–31782

Winayanuwattikun, P. and Ketterman, J.A., (2007). A Newly Identified Residue of The Functionally Conserved Electron Sharing Network Contributes To Catalysis and Structural Integrity of Glutathione Transferases. Biochemical Journal, 402: 339–348

Wongsantichon, J., Robinson, R.C. and Ketterman, A.J. (2010). Structural Contributions of Delta Class Glutathione Transferase Active-Site Residues to Catalysis. Biochemical Journal, 428: 25–32

Wongsantichon, J., Robinson, R.C. and Ketterman, A.J. (2012). Structural Evidence for Conformational Changes of Delta Class Glutathione Transferases after Ligand Binding. Archives of Biochemistry and Biophysics, 521 (1–2): 77–83

Wongtrakul, J., Udomsinprasert, R. and Ketterman, A.J. (2003). Non-Active Site Residues Cys69 and Asp150 Affected the Enzymatic Properties of Glutathione S-Transferase Adgstd3-3. Insect Biochemistry and Molecular Biology, 33: 971–979

Wongtrakul, J., Wongsantichon, J., Vararattanavech, A., Leelapat, P., Prapanthadara, L. and Ketterman, A.J. (2009). Molecular Cloning and Expression of Several New *Anopheles cracens* Epsilon Class Glutathione Transferases. Protein & Peptide Letters, 16: 75-81.

Yamamoto, K., Ichinose, H., Aso, Y., Banno,Y., Kimura, M. and Nakashima, T. (2011). Molecular Characterization of an Insecticide-Induced Novel Glutathione Transferase in Silkworm. Biochimica et Biophysica Acta, 1810: 420–426

Yang, J., McCart, C., Woods, D.J., Terhzaz, S., Greenwood, K.G., Constant, R.H.F. and Dow, J.A.T. (2007). A *Drosophila* Systems Approach to Xenobiotic Metabolism. Physiology Genomics, 30: 223-231